

Studies of Electromagnetic Transitions in B^{11} and $C^{11}\dagger$

J. W. OLNES, E. K. WARBURTON, D. E. ALBURGER, AND J. A. BECKER*

Brookhaven National Laboratory, Upton, New York

(Received 16 March 1965)

Electromagnetic transitions in B^{11} and C^{11} have been investigated through the reactions induced (a) by He^9 bombardment of Be^9 targets and (b) by deuteron bombardment of B^{10} targets employing bombarding energies ranging from 2.0 to 3.5 MeV. Branching ratios for the decay of the bound levels of B^{11} populated in (a) and (b) by the $Be^9(He^3,p)B^{11*}$ and $B^{10}(d,p)B^{11*}$ reactions were determined through measurements of proton-gamma coincidence spectra. The ratios of radiative width to total width for the unbound 9.19- and 8.92-MeV levels of B^{11} were obtained as $\Gamma_\gamma/\Gamma(9.19)=0.1_{-0.05}^{+0.2}$ and $\Gamma_\gamma/\Gamma(8.92)=1.08\pm 0.12$. Additional measurements of the direct gamma spectra employing a three-crystal NaI(Tl) pair spectrometer, and of the internal pair transitions using an intermediate-image magnetic spectrometer, complement the above results and provide information on the decay of those bound levels of C^{11} populated by the $Be^9(He^3,n)C^{11*}$ and $B^{10}(d,n)C^{11*}$ reactions. The angular distributions of gamma rays from the four listed reactions were measured with the three-crystal pair spectrometer, and indicate significant anisotropies for those gamma rays arising from decay of the 8.92- and 7.99-MeV levels of B^{11} and the 7.50-MeV level of C^{11} formed in the Be^9+He^9 bombardment. From the Doppler shifts apparent in the angular-distribution data an upper limit of $\tau < 5 \times 10^{-13}$ sec was extracted for the mean lifetime of all bound levels of B^{11} and C^{11} except the 6.81-MeV level of B^{11} , which could not be studied in this manner. The intermediate-image spectrometer was used to determine the multipolarity of those internal pair transitions in B^{11} and C^{11} having transition energies greater than 4 MeV. These results show that the 7.99- and 7.30-MeV levels of B^{11} and the 7.50-, 6.90-, and 6.35-MeV levels of C^{11} decay by $E1$ ground-state transitions and hence have even parity, while the 8.92- and 6.76-MeV levels of B^{11} and 6.49-MeV level of C^{11} decay by $M1$ and/or $E2$ ground-state transitions, and hence have odd parity. Combining these results with previously available information leads to spin-parity assignments of $\frac{5}{2}^-$ and $\frac{3}{2}^+$ for the 8.92- and 7.99-MeV levels of B^{11} , respectively, and strongly suggests the assignment $\frac{3}{2}^+$ for the 7.50-MeV level of C^{11} . The odd-parity assignment to the 2.14-MeV level of B^{11} is confirmed while the parity of the C^{11} 2.00-MeV level is fixed as odd. For the remaining levels the measurements serve to further restrict the range of possible spin-parity assignments. In addition the parities of the Be^{11} ground state and B^{11} 6.81-MeV level are determined to be even since the beta decay of Be^{11} to the B^{11} $\frac{3}{2}^+$ 7.99-MeV level and the 6.81-MeV level are known to be allowed. The level schemes of B^{11} and C^{11} as deduced from the present results are discussed in terms of the predictions of the intermediate-coupling shell model and the weak-coupling scheme.

I. INTRODUCTION

THE work reported in this paper was undertaken to obtain information on the spins and parities of the bound energy levels of B^{11} and C^{11} and on the multipolarities of the gamma-ray transitions connecting them. The current state of knowledge on the energy levels of these two nuclei is illustrated by the energy-level diagram shown in Fig. 1 which shows the known B^{11} levels below 9.8-MeV excitation and the known C^{11} levels below 8.8-MeV excitation. The information concerning B^{11} is taken mainly from the review of Lauritsen and Ajzenberg-Selove.¹ The excitation energies for B^{11} are all known to better than ± 10 keV.² Some of the B^{11} spin-parity assignments in Fig. 1 are different from those given by Lauritsen and Ajzenberg-Selove.¹ A definite spin-parity assignment has been made to the 6.76-MeV level. The spin assignment comes from the work of Green, Stephens, and Willmott,³ while the

parity assignment comes from that work and also from the various stripping results^{1,2} which are in good agreement with $l_n=1$ neutron transfer in the $B^{10}(d,p)B^{11}$ reaction. The B^{11} 6.81-MeV level is given an assignment of $(\frac{1}{2}, \frac{3}{2})^+$, the parity coming from the recent work^{4,5} on the beta decay of Be^{11} . There seems to be no experimental evidence which favors $\frac{3}{2}^+$ over $\frac{1}{2}^+$. The tentative assignment of $J=\frac{5}{2}$ for the 7.30-MeV level has been removed since that assignment seems to have been suggested⁶ to conform with theoretical shell-model predictions⁷ and not experimental evidence.

The excitation energies of the C^{11} levels are all known to ± 10 keV or better^{2,8} except for the level at 8.70 MeV which is known to ± 20 keV.⁹ The information on the spin-parity assignments to the C^{11} states is mostly quite recent. The ground state has recently been shown to have $J=\frac{3}{2}$ by the atomic beam resonance technique.¹⁰

⁴ D. H. Wilkinson and D. E. Alburger, Phys. Rev. **113**, 563 (1959).

⁵ D. E. Alburger, C. Chasman, K. W. Jones, J. W. Olnes, and R. A. Ristinen, Phys. Rev. **136**, B916 (1964).

⁶ A. J. Ferguson, H. E. Gove, J. A. Kuehner, A. E. Litherland, E. Almqvist, and D. A. Bromley, Phys. Rev. Letters **1**, 414 (1958).

⁷ D. Kurath, Phys. Rev. **106**, 975 (1957).

⁸ S. Hinds and R. Middleton, Proc. Phys. Soc. (London) **78**, 81 (1961).

⁹ J. C. Overley, Nucl. Phys. **49**, 537 (1963).

¹⁰ J. L. Snider, M. Posner, A. M. Bernstein, and D. R. Hamilton, Bull. Am. Phys. Soc. **6**, 244 (1961); R. A. Haberstroh, W. J. Kossler, O. Ames, and D. R. Hamilton, Phys. Rev. **136**, B932 (1964).

[†] Work performed under the auspices of the U. S. Atomic Energy Commission.

* Present address: Lockheed Missiles and Space Company, Palo Alto, California.

¹ T. Lauritsen and F. Ajzenberg-Selove, *Nuclear Data Sheets*, compiled by K. Way *et al.* (Printing and Publishing Office, National Academy of Sciences—National Research Council, Washington, D. C., 1962), Sets 5 and 6.

² F. Ajzenberg-Selove and T. Lauritsen, Nucl. Phys. **11**, 1 (1959).

³ L. L. Green, G. A. Stephens, and J. C. Willmott, Proc. Phys. Soc. (London) **79**, 511 (1962).

Negative parity is assigned to the ground state as a result of analysis of the pickup reaction¹¹ C¹²(*p,d*)C¹¹ and the stripping reactions^{1,2,8,9} B¹⁰(He³,*d*)C¹¹ and B¹⁰(*d,n*)C¹¹. The spin-parity assignments made to the levels at 4.32, 4.81, 6.49, 8.43, 8.66, and 8.70 MeV are also based on the observations on the angular distributions in the B¹⁰(He³,*d*)C¹¹ and B¹⁰(*d,n*)C¹¹ reactions. A spin assignment of $\frac{1}{2}$ is ruled out for the C¹¹ 4.32- and 6.49-MeV levels by the B¹⁰(*p, γ)C¹¹ results of James.¹² The C¹¹ 2.00-MeV level is assigned a most probable spin of $\frac{1}{2}$ from results obtained¹³ using the C¹²(He³, α)C¹¹ reaction. The (*d,n*) and (He³,*d*) stripping patterns indicate $l_n=1$ for the reactions leading to the C¹¹ 2.00-MeV level; however, the analysis is less reliable than usual since a mechanism such as "spin-flip" stripping¹⁴ must be invoked in order to explain the results.*

The primary motive for undertaking a study of the electromagnetic transitions in mass 11 was to determine the parities of the B¹¹ 7.30-, 7.99-, 8.57-, and 8.92-MeV levels and the C¹¹ 2.00-, 6.35-, 6.90-, and 7.50-MeV levels. For all other bound excited states of B¹¹ and C¹¹, except the B¹¹ 2.14-MeV level, the parity measurements have been made by analysis of single or double stripping reactions. This method either failed or gave inconsistent results for the levels listed above. Furthermore, the determination of parities by analysis of direct reactions is model dependent and therefore never absolutely reliable. Thus, when possible, it is desirable to confirm the parity assignments made from analysis of direct reaction angular distributions by a more rigorous method.

The method we have used to assign parities to the mass-11 levels is that of studying the angular correlation of the internal pairs emitted in competition with gamma rays in electromagnetic transitions with energies greater than 2 MeV, using an intermediate-image pair spectrometer to detect the pairs. The determination of the multipolarity of electromagnetic transitions with this spectrometer has been described previously.^{15,16} The reactions used to populate the B¹¹ and C¹¹ levels were Be⁹(He³,*p*)B¹¹ ($Q=10.325$ MeV), Be⁹(He³,*n*)C¹¹ ($Q=7.560$ MeV), B¹⁰(*d,p*)B¹¹ ($Q=9.231$ MeV), and B¹⁰(*d,n*)C¹¹ ($Q=6.466$ MeV). Bombarding energies between 2.0 and 3.5 MeV were used so that all the B¹¹ and C¹¹ levels shown in Fig. 1 were populated during the course of this work. However, we did not observe gamma rays from the decay of the B¹¹ 9.28-MeV level and the C¹¹ levels between the threshold for

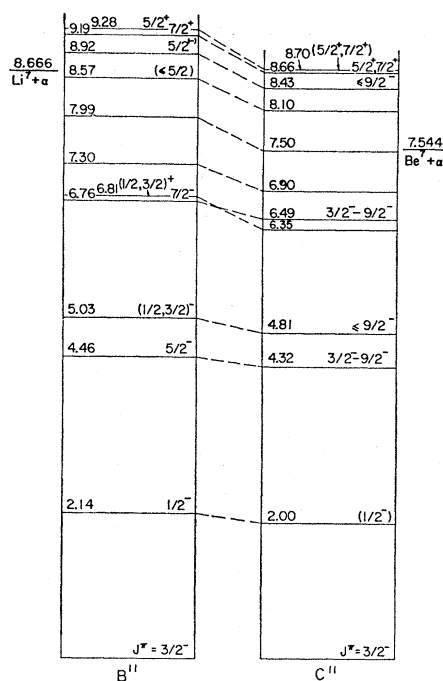


Fig. 1. Energy-level diagrams for B¹¹ and C¹¹, illustrating the excitation energies and spin-parity assignments as reported from previous measurements. The information is taken primarily from the review of Lauritsen and Ajzenberg-Selove (Ref. 1) but incorporates the results of later measurements as explained in the text. Uncertain spin-parity assignments are enclosed in parentheses. Suspected mirror levels in B¹¹ and C¹¹ are connected by dashed lines.

α -particle decay (7.544 MeV) and the threshold for proton emission (8.691 MeV). This is presumably because, for these states, the gamma-ray width Γ_γ is negligibly small compared to the α -particle width Γ_α .

Our experimental investigations of electromagnetic transitions in B¹¹ and C¹¹ are described in the next three sections. In Sec. II is described a determination of the decay modes of the B¹¹ states below 9-MeV excitation by two-dimensional analysis of the Be⁹(He³,*p γ*)B¹¹ and B¹⁰(*d,p γ*)B¹¹ reactions. In Sec. III we present the results of three-crystal pair spectrometer studies of the gamma rays emitted in the Be⁹(He³,*p γ*)B¹¹, Be⁹(He³,*n γ*)C¹¹, B¹⁰(*d,p γ*)B¹¹, and B¹⁰(*d,n γ*)C¹¹ reactions. Finally, the results obtained in the study of the internal pairs emitted following the four reactions listed above are given in Sec. IV.

II. PROTON-GAMMA COINCIDENCE STUDIES

A. Procedures

The gamma-ray decays of the levels of B¹¹ up to and including the 9.28-MeV level have been investigated principally via the Be⁹(He³,*p γ*)B¹¹ reactions,^{6,17} the

¹¹ C. D. Kavaloski, G. Bassani, and N. M. Hintz, Phys. Rev. **132**, 813 (1963).

¹² A. N. James, Nucl. Phys. **24**, 675 (1961).

¹³ E. K. Warburton, J. S. Lopes, R. W. Ollerhead, A. R. Poletti, and M. F. Thomas, Phys. Rev. **138**, B104 (1965).

¹⁴ D. H. Wilkinson, Phys. Rev. **105**, 666 (1957); N. T. S. Evans and A. P. French, *ibid.* **109**, 1272 (1958); J. C. Hensel and W. C. Parkinson, *ibid.* **110**, 128 (1958).

¹⁵ E. K. Warburton, D. E. Alburger, A. Gallmann, P. Wagner, and L. F. Chase, Jr., Phys. Rev. **133**, B42 (1964).

¹⁶ E. K. Warburton, J. W. Olness, D. E. Alburger, D. J. Bredin, and L. F. Chase, Jr., Phys. Rev. **134**, B338 (1964).

¹⁷ P. F. Donovan, J. V. Kane, R. E. Pixley, and D. H. Wilkinson, Phys. Rev. **123**, 589 (1961).

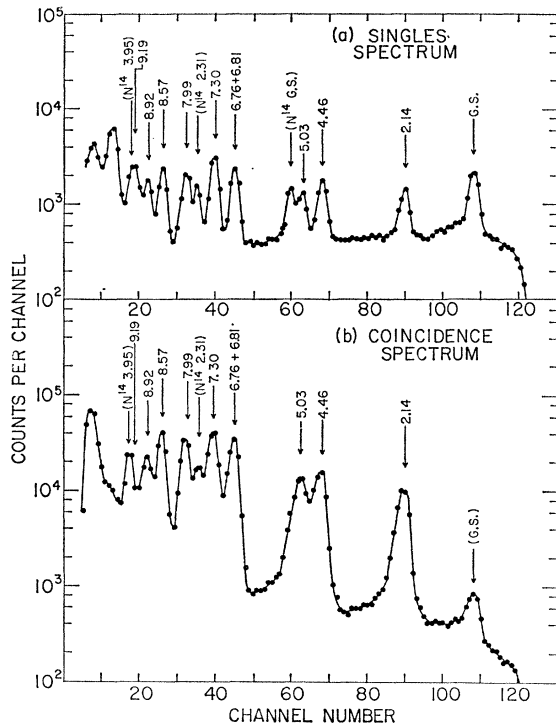


FIG. 2. Pulse-height spectra of charged particles from 2.0-MeV He^3 bombardment of a Be^9 target. The data were recorded with a silicon surface-barrier detector at 70° to the He^3 beam. Proton groups from the $\text{Be}^9(\text{He}^3, p)\text{B}^{11}$ reaction are identified by the excitation energies (in MeV) of the B^{11} levels to which they correspond. Proton groups from $\text{C}^{12}(\text{He}^3, p)\text{N}^{14}$ are also apparent and are similarly identified. The singles spectrum is shown in the upper plot, while the lower plot shows the spectrum measured in coincidence with all gamma rays corresponding to $E_\gamma > 0.4$ MeV.

$\text{Li}^7(\alpha, \gamma)\text{B}^{11}$ reaction,^{3,18} and the beta decay^{4,5} of Be^{11} . We have re-examined these results through 2-parameter analysis of the $\text{Be}^9(\text{He}^3, p)\text{B}^{11}$ and $\text{B}^{10}(d, p)\text{B}^{11}$ reactions. Our results confirm the major features of the earlier measurements, and serve also to clear up some of the uncertainties attached to the weaker decay modes.

The proton-gamma coincidence measurements were carried out using thin targets of Be^9 or B^{10} located at the center of a cylindrical scattering chamber with an angle of 45° between the normal to the target face and the incident beam direction. Final collimation of the charged-particle beam from the Van de Graaff accelerator was achieved by a 1-mm-diam tantalum aperture located at the chamber entrance. Charged reaction products were detected using a silicon surface barrier counter placed at 70° to the incident beam direction and at a distance of 1.5 cm from the reaction site ($\varphi = 0^\circ$). The angular spread of the reaction products was limited to $\Delta\theta \approx 10^\circ$ by a set of tantalum slits at the detector face. Gamma rays were detected by a 5×5 -in.

NaI(Tl) crystal placed directly above the target ($\varphi = 90^\circ$) at a distance of 2 cm from the target. The cover plate of the scattering chamber was made from lucite and cut out to a thickness of $\frac{1}{4}$ in. between the target and gamma-ray detector in order to minimize absorption effects. Coincident amplified pulses from the gamma detector and the proton detector were recorded by a TMC 16 384-channel 2-parameter analyzer used in its 128×128 -channel mode. The necessary coincidence conditions were imposed by an external coincidence circuit ($\tau = 100$ nsec) which gated the 2-parameter analyzer.

Coincidence data on the $\text{Be}^9(\text{He}^3, p\gamma)\text{B}^{11}$ reaction were obtained in a single run of ~ 20 h at a bombarding energy of 2.0 MeV and a He^3 current of $0.03 \mu\text{A}$. The target was a $50 \mu\text{g}/\text{cm}^2$ self-supporting foil prepared by vacuum evaporation of beryllium powder. A $3 \text{ mg}/\text{cm}^2$ aluminum absorber was used to prevent elastically scattered He^3 from reaching the detector.

The $\text{B}^{10}(d, p\gamma)\text{B}^{11}$ measurements were carried out at a deuteron bombarding energy of 2.0 MeV and a beam current of $\sim 0.05 \mu\text{A}$. The target in this case was a self-supporting foil of B^{10} with an area density of ~ 50

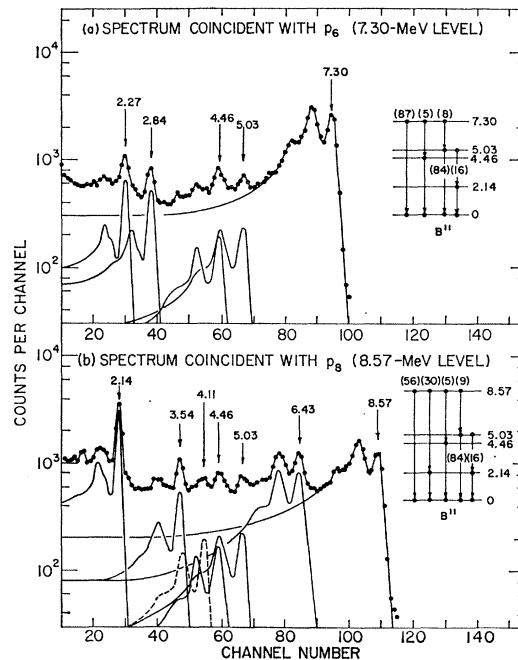


FIG. 3. Proton-gamma coincidence spectra illustrating the decay modes of the B^{11} 7.30- and 8.57-MeV levels populated in the $\text{Be}^9(\text{He}^3, p)\text{B}^{11}$ reaction. The data were recorded simultaneously through 2-parameter analysis of pulses from the 5×5 -in. NaI(Tl) gamma-ray detector and a solid-state particle detector. The upper plot (a) shows the gamma-ray spectrum measured in coincidence with the p_6 group leading to the B^{11} 7.30-MeV level. The spectrum has been resolved into the indicated component gamma rays, arising from de-excitation of the 7.30-MeV level to the ground state, 4.46- and 5.03-MeV levels of B^{11} , as indicated in the level diagram shown in the inset. A similar plot is shown in (b) for the 8.57-MeV level, illustrating the component gamma rays arising from de-excitation of this level to the ground state and to the 2.14-, 4.46-, and 5.03-MeV levels of B^{11} .

¹⁸ G. A. Jones, C. M. P. Johnson, and D. H. Wilkinson, *Phil. Mag.* **43**, 796 (1959).

$\mu\text{g}/\text{cm}^2$. The coincidence data were acquired in a run of about 20 h.

B. Results

The $\text{Be}^9(\text{He}^3, p\gamma)\text{B}^{11}$ Reaction

Figure 2(a) shows the proton singles spectrum obtained under the same conditions that prevailed for the coincidence measurements shown in Fig. 2(b). The various proton groups from the $\text{Be}^9(\text{He}^3, p\gamma)\text{B}^{11}$ reaction are designated by the B¹¹ level energies, given in MeV. The first three groups (p_0, p_1, p_2) from the $\text{C}^{12}(\text{He}^3, p)\text{N}^{14}$ reaction are also evident. The "continuum" underlying the labeled proton peaks arises primarily from the $\text{Be}^9(\text{He}^3, \alpha)\text{Be}^{8*} \rightarrow 2\alpha$ reaction.

Figure 2(b) shows the proton spectrum measured in coincidence with all gamma rays of pulse height corresponding to $E_\gamma \geq 0.4$ MeV. The N¹⁴ ground-state group is no longer apparent, while the B¹¹ ground-state group is depressed by a factor of at least 10. Since a large fraction of the random coincidences arise from the presence of intense annihilation radiation, the actual ratio of real-to-randoms for $E_\gamma > 1$ MeV is 20:1 or better. Of course the single-parameter presentation of Fig. 2(b) illustrates only a fraction of the information available from the 2-parameter data output. It is also possible to examine the individual gamma-ray spectra in coincidence with the various proton groups, as is shown in Fig. 3 for two of the more complex decay

TABLE I. B¹¹ branching ratios from the $\text{Be}^9(\text{He}^3, p\gamma)\text{B}^{11}$ and $\text{B}^{10}(d, p\gamma)\text{B}^{11}$ reactions.

Initial state (MeV)	Final state (MeV)	E_γ (MeV)	Branching ratios (%)		
			$\text{Be}^9 + \text{He}^3$	$\text{B}^{10} + d$	Average
4.46	0	4.46	100	100	100
	2.14	2.32	<1	<1	<1
5.03	0	5.03	84±2	85±3	84±2
	2.14	2.89	16±2	15±1	16±2
6.76	0	6.76	(59±8)	71±2	71±2
	2.14	4.62	<3	<3	<3
	4.46	2.30	(41±8)	29±2	29±2
	5.03	1.73	<1	<1	<1
6.81	0	6.81	65±8	65±8	65±8
	2.14	4.67	35±8	35±8	35±8
	4.46	2.35	<8	<8	<8
	5.03	1.78	<8	<8	<8
7.30	0	7.30	87±2	87±2	87±2
	2.14	5.16	<1.5	<1	<1
	4.46	2.84	5±1	6±1	5.5±1
7.99	5.03	2.27	8±1	7±1	7.5±1
	0	7.99	46±2	49±2	47±2
	2.14	5.85	54±2	51±2	53±2
	4.46	3.53	<1	<1	<1
8.57	5.03	2.96	<1	<1	<1
	0	8.57	56±2	56±2	56±2
	2.14	6.43	30±2	30±2	30±2
	4.46	4.11	5±1	5±1	5±1
8.92	5.03	3.54	9±1	9±1	9±1
	0	8.92	96±1	95±1	95±1
	2.14	6.78	<2	<1	<1
	4.46	4.46	4±0.5	5±0.5	5±0.5
	5.03	3.89	<2	<1	<1
6.76	2.16	<2	<1	<1	

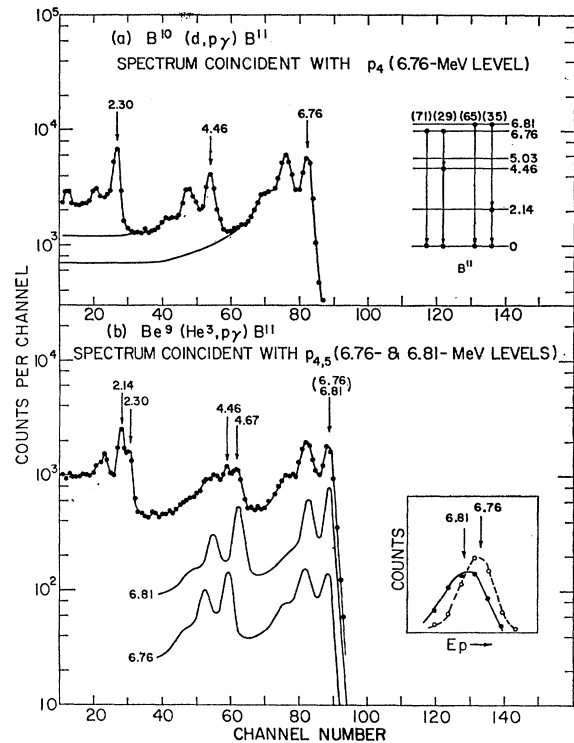


FIG. 4. Proton-gamma ray coincidence spectra illustrating the decay modes of the 6.76- and 6.81-MeV levels of B¹¹. The gamma-ray spectrum measured in coincidence with the p_4 group from $\text{B}^{10}(d, p\gamma)\text{B}^{11}$ is shown in (a) while the spectrum measured in coincidence with the experimentally unresolved p_4 and p_5 groups from the $\text{Be}^9(\text{He}^3, p\gamma)\text{B}^{11}$ reaction is shown in (b). The proton spectra measured in coincidence with the 4.46- and 4.67-MeV gamma-ray peaks are shown in the inset, showing the presence of both the p_4 and p_5 groups. The decomposition of the 2-parameter data to yield the gamma-ray spectra in coincidence with the individual p_4 and p_5 groups is shown by the solid curves of (b). The decay schemes and branching ratios thus deduced from both (a) and (b) for the 6.76- and 6.81-MeV levels is also indicated.

schemes examined, i.e., for the decays of the 7.30- and 8.57-MeV levels of B¹¹. These data were obtained by summing the data matrix over a number of proton channels corresponding roughly to the full width at half-maximum of a given peak in the proton distribution. The data analysis was facilitated by utilizing a computer program to carry out the various summing operations required for examination of the data. The relatively simple decay of the 2.14-, 4.46-, 7.99-, and 8.92-MeV levels permitted a determination of the energy dependence of the detector response, i.e., line shape and peak efficiency as a function of gamma-ray energy. The total efficiency as a function of gamma energy was taken from Vegors, Marsden, and Heath.¹⁹

Figure 3(a) shows the gamma-ray spectrum coincident with protons leading to the 7.30-MeV level of B¹¹. In addition to the strong ground-state transition, the gamma-rays arising from the cascade transitions

¹⁹ S. H. Vegors, Jr., L. L. Marsden, and R. L. Heath, Phillips Petroleum Company, Atomic Energy Division, IDO 16370, 1958 (unpublished).

7.30 \rightarrow 4.46 and 7.30 \rightarrow 5.03 are also evident. The spectrum was decomposed by peeling off the various components, using for this purpose the line shapes determined from the less complex decays. The components thus identified are also indicated in Fig. 3(a). The branching ratios calculated from these results, after corrections for summing, are given in Table I.

A similar plot for the 8.57-MeV level is shown in Fig. 3(b). The decomposition of the gross spectrum into the various components arising from transitions from the 8.57-MeV level to the ground state, 2.14-, 4.46-, and 5.03-MeV levels is illustrated. The decay scheme is shown in the insert, and the branching ratios are given in Table I.

Similar procedures were carried out for the 5.03-, 7.99-, and 8.92-MeV levels, with the results shown in Table I. The determination of the decay schemes for the 6.76- and 6.81-MeV levels was complicated since the resolution of the proton detector was not good enough to separate the proton groups leading to these two levels, as is evident from the singles proton spectrum shown in Fig. 2(a). The gamma-ray spectrum in coincidence with this doublet peak is shown in Fig. 4(b). However, the pulse-height distributions of protons in coincidence (a) with the 2.30- and 4.46-MeV gamma-ray photopeaks and (b) with the 4.67- and 2.14-MeV gamma-ray photopeaks exhibit two distinct peaks, corresponding in energy to the proton groups leading respectively to the 6.76- and 6.81-MeV levels of B^{11} . This is shown in the insert of Fig. 4(b). Therefore, by comparing quantitatively the gamma-ray spectra associated with the "high"- and "low"-energy sides of this doublet it was possible to determine the gamma-ray spectra arising from the decay of the individual 6.76- and 6.81-MeV levels, as is shown by the solid curves of Fig. 4(b). The branching ratios calculated from the two curves unfolded in this manner are given in Table I; the relatively larger errors attached to these reflect the uncertainties involved in the unfolding process.

The $B^{10}(d,p\gamma)B^{11}$ Reaction

These data were treated in the same fashion as the $Be^9(He^3,p)B^{11}$ data. The results are summarized in Table I. The 8.57- and 6.81-MeV levels are not strongly fed in the (d,p) reactions, and no information is gained on these levels. For the remaining levels at 2.14, 4.46, 5.03, 7.30, 7.99 and 8.92 MeV the results provide a satisfactory check of those obtained from the $Be^9(He^3,p\gamma)B^{11}$ measurements, and accordingly, the final values for the branching ratios are taken as an average of the two measurements. The (d,p) data are particularly useful for determining the branching of the 6.76-MeV level. The gamma-ray spectrum is presented in Fig. 4(a) for comparison with that obtained in Fig. 4(b) from the $Be^9(He^3,p\gamma)B^{11}$ reaction. From the absence of the 4.67- and 2.14-MeV lines, we can place an upper limit of 8% on the feeding of the 6.81-MeV

state. Hence, the most accurate determination of the 6.76-MeV level branching ratios are obtained from the data of Fig. 4(a) and are given in Table I. The results are seen to be in reasonable agreement with those obtained from the $Be^9(He^3,p\gamma)B^{11}$ measurements.

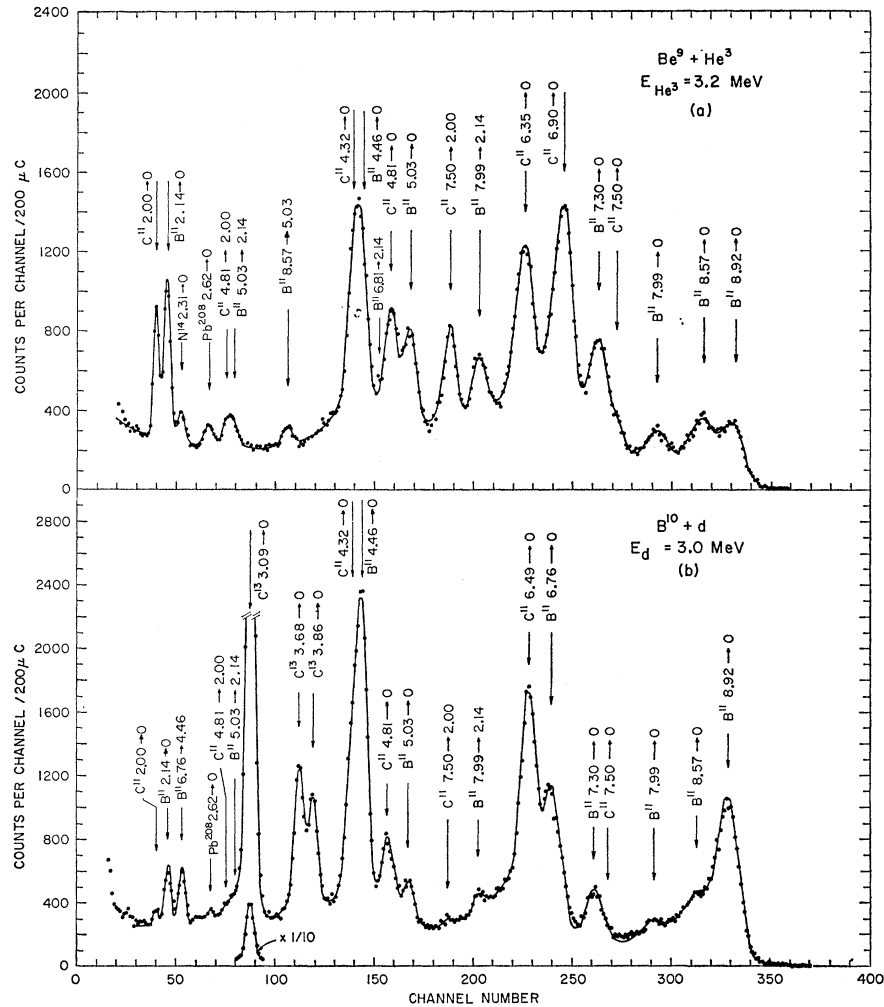
The branching ratios of B^{11} determined using the $B^{10}(d,p)B^{11}$ and $Be^9(He^3,p)B^{11}$ reactions are in substantial agreement with each other and with the branching ratios determined from the 3-crystal pair spectrometer data described in Sec. III. This agreement indicates that the effects of anisotropies in the proton-gamma correlations are small in both geometries. This is expected since for the geometry used the $P_2(\cos\theta)$ and $P_4(\cos\theta)$ attenuation coefficients are ~ 0.4 and ~ 0.08 , respectively, and, in any case, any deviations from isotropy for the gamma-ray detector at right angles to the reaction planes are expected to be small (identically zero for the plane-wave theory of direct reactions).

Determination of (Γ_γ/Γ) for the 8.92- and 9.19-MeV Levels of B^{11}

The ratio of radiation width to total width for the 8.92-MeV level is readily obtained from the proton singles spectrum of Fig. 2(a) and from the gamma-ray coincidence spectra associated with the 8.92-MeV proton peak.

Designating the total gamma-ray intensity observed in coincidence as $I_\gamma(8.92)$, and the proton intensity observed in the singles spectrum of Fig. 2(a) as $I_p(8.92)$, we can write $\Gamma_\gamma/\Gamma(8.92) = [I_\gamma(8.92)/I_p(8.92)] / [I_\gamma(b)/I_p(b)]$ where the symbol b designates the corresponding quantities for some (any) bound level. We have chosen the above form to calculate $\Gamma_\gamma/\Gamma(8.92)$, utilizing the fact that $\Gamma_\gamma/\Gamma(b) \equiv 1$, since it does not require one to know the normalizing factors which must obtain between singles and coincidence spectra. The ratios indicated above were calculated for the 8.92-MeV level, and for both of the two bound levels at 8.57 and 7.99 MeV. The results provide a satisfactory internal check on the procedure, yielding the value $\Gamma_\gamma/\Gamma(8.92) = 1.06 \pm 0.15$. From the $B^{10}(d,p\gamma)B^{11}$ data, where it is most convenient to compare the 8.92- and 6.76-MeV states, we obtain the result $\Gamma_\gamma/\Gamma(8.92) = 1.10 \pm 0.15$. We adopt the value $\Gamma_\gamma/\Gamma(8.92) = 1.08 \pm 0.12$, and set an upper limit on the radiative width of the 8.92-MeV state of $\Gamma_\gamma/\Gamma(8.92) \geq 0.96, 0.84, \text{ and } 0.72$ to 1, 2, and 3 standard deviations. A similar approach applied to the determination of the radiative width of the B^{11} 9.19-MeV level yields the result $\Gamma_\gamma/\Gamma(9.19) = 0.1_{-0.05}^{+0.2}$. The $+0.2$ error reflects primarily the uncertainty involved in unfolding the B^{11} p_{11} (9.28-MeV level) contribution to the singles spectrum of Fig. 2(a). The results indicate the levels are populated in the ratio $(9.19/9.28) \simeq \frac{3}{2}$. Since $\Gamma_\gamma/\Gamma(9.28) \cong 0$, the possible influence of this level on the $p\gamma$ coincidence spectra of Fig. 2(b) is negligibly small. On the other hand, contributions due to the $N^{14}p_2$ (3.95-MeV level) group from

FIG. 5. Gamma-ray pulse-height spectra measured with a 3-crystal pair spectrometer (a) from He³ bombardment of a Be⁹ target and (b) from deuteron bombardment of a B¹⁰ target. Transitions originating from levels of B¹¹ and C¹¹ populated by the Be⁹(He³,p)B¹¹ and Be⁹(He³,n)C¹¹ reactions are indicated in (a) by the energies (in MeV) of the initial and final nuclear levels between which the transitions occur. A similar plot is shown in (b) illustrating the transitions originating from levels of B¹¹ and C¹¹ populated in the B¹⁰(d,p)B¹¹ and B¹⁰(d,n)C¹¹ reactions. The effects of carbon contamination of both the Be⁹ and B¹⁰ targets are evident in (a) and (b) through the presence of peaks identified with the C¹²(He³,p)N¹⁴ and C¹²(d,p)C¹³ reactions, respectively. The 2.62-MeV peak arises primarily from inelastic scattering of neutrons in the lead shielding the pair spectrometer. These data were obtained at an angle $\theta_s = 90^\circ$ as part of the angular-distribution measurements described in the text. The solid curves through the experimental points are the result of a computer fit to the data which was employed to determine gamma-ray intensities.



C¹²(He³,p)N¹⁴ were readily estimated, following the method described previously for the B¹¹ 6.76-, 6.81-MeV doublet.

III. GAMMA-RAY ANGULAR-DISTRIBUTION MEASUREMENTS

A. Procedures

A 3-crystal pair spectrometer, described previously,¹⁶ was used for the gamma-ray angular-distribution measurements. In this design the three NaI(Tl) detectors of the spectrometer are fixed in a lead shield mounted on a rotating platform which provides automatic alignment of the viewing axis and the axis of rotation. The procedures for aligning the spectrometer with respect to the target have also been described previously.¹⁶ For the measurements reported here, the front face of the central detector (1½-in. × 3-in. NaI(Tl)) was located at a distance of 10 cm from the target center. The over-all gain of each detector was monitored by a stabilizer operating on the 835-keV photopeak produced by Mn⁵⁴ sources located in the vicinity of the crystals. Targets

of both Be⁹ and B¹⁰ were prepared in the form of thin foils and were positioned in a cylindrical target chamber with an angle of 45° between the normal to the target face and the incident beam direction, thus minimizing the effects of gamma-ray absorption in the target itself. Amplified pulses from the central detector were recorded by a 400-channel RIDL analyzer, which was gated with a standard coincidence circuit which imposed the necessary triple coincidence requirements. It has been previously estimated that the net uncertainty introduced in the experimental measurements by geometric misalignment or electronic instability is limited with the arrangement described above to less than 1%.

Spectra were measured for several bombarding energies ranging from 2.5 to 3.5 MeV for both the Be⁹+He³ and B¹⁰+d reactions. The results exhibit no readily discernible resonance structure, although the yield does show a general increase with bombarding energy, particularly for the higher energy transitions. Angular distribution measurements were therefore made at E_d=3.0 MeV for B¹⁰+d and E_{He³}=3.2 MeV for Be⁹+He³, these energies being selected to give maxi-

TABLE II. Relative intensities and angular distribution coefficients from 3-crystal pair spectrometer measurements.

E_γ (MeV)	Assignment	Be ⁹ +He ³			B ¹⁰ +d		
		I_γ (arbitrary units)	a_2 (%)	a_4 (%)	I_γ (arbitrary units)	a_2 (%)	a_4 (%)
8.92	B ¹¹ 8.92 → 0	50±3	-10±3	2±3	164±9	-5±3	0±3
8.57	B ¹¹ 8.57 → 0	36±3	5±4	-1±5	30±3		
7.99	B ¹¹ 7.99 → 0	26±2	10±5	-4±5	16±3		
7.50	C ¹¹ 7.50 → 0	32±6	12±10	-9±12	W		
7.30	B ¹¹ 7.30 → 0	70±5	-10±5	6±6	57±3	1±4	-2±5
6.90	C ¹¹ 6.90 → 0	152±8	-3±2	2±2	W		
6.81	B ¹¹ 6.81 → 0	W			No		
6.76	B ¹¹ 6.76 → 0	W			136±8	5±3	-1±4
6.49	C ¹¹ 6.49 → 0	W			188±10	6±3	4±4
6.35	C ¹¹ 6.35 → 0	105±6	1±2	1±2	No		
5.86	B ¹¹ 7.99 → 2.14	28±2	-14±4	2±4	12±2		
5.50	C ¹¹ 7.50 → 2.00	37±2	-13±3	-1±3	4±1		
5.03	B ¹¹ 5.03 → 0	46±4	1±3	-1±3	32±2	-3±4	-1±5
4.81	C ¹¹ 4.81 → 0	51±3	2±3	2±3	60±3	-2±3	0±4
4.67	B ¹¹ 6.81 → 2.14	9±2			No		
4.46	B ¹¹ 4.46 → 0	60±4	-2±5	-8±6	180±10	-3±4	2±4
4.32	C ¹¹ 4.32 → 0	70±5	0±6	12±7	99±6	10±6	0±7
	C ¹¹ 6.35 → 2.00						
3.54	B ¹¹ 8.57 → 5.03	6±1			W		
2.93	B ¹¹ 5.03 → 2.14	11±2			13±4		
2.83	C ¹¹ 4.81 → 2.00	15±2			9±4		
2.58	C ¹¹ 6.90 → 4.32	(15±2) ^a			(7±3) ^a		
2.30	B ¹¹ 6.76 → 4.46	(21±2) ^b			51±8		
2.14	B ¹¹ 2.14 → 0	120±7	1±3	1±3	56±10		
	C ¹¹ 6.49 → 4.32						
2.00	C ¹¹ 2.00 → 0	108±7	5±4	1±4	28±8		

^a Contains an unknown contribution from Pb²⁰⁸ 2.62 → 0.

^b Contains a large contribution from N¹⁴ 2.31 → 0.

mum yield consistent with stable, reliable operation of the Van de Graaff accelerator. Data were recorded for both reactions for 5 angles of observation ($\theta=0, 30, 45, 60,$ and 90 deg) with respect to the incident beam direction. The reaction-gamma flux was monitored during these measurements by a 3-in.×3-in. NaI(Tl) detector, which also provided a check on the possible effects of target deterioration and target nonuniformity.

The Be⁹ target was a thin (0.001-in.) beryllium foil placed on a tantalum backing which served to stop the He³ beam. The target showed no measurable deterioration under prolonged bombardments of $\sim 0.04 \mu\text{A}$, and hence the spectra measured at the various angles were normalized to the total integrated charge deposited by the incident beam, as determined by a current integrator. It is estimated that the net uncertainty introduced into these angular-distribution measurements by experimental errors is $< 2\%$.

For the B¹⁰+d measurements the target was prepared by mixing B¹⁰ powder with an aqueous suspension of carbon, and then making a self-supporting foil from this mixture. This target was neither as uniform nor as stable as the Be⁹ target, showing measurable deterioration under bombardment of about $0.003 \mu\text{A}$. It is estimated that the net experimental uncertainty is about 2.5%, and is limited primarily by the accuracy with which the net monitor counts (minus background) were recorded.

The spectra recorded at $\theta=90^\circ$ for both the B¹⁰+d

and Be⁹+He³ measurements are shown in Fig. 5. The solid curves are the results of a computer fit to the data which was used in the angular-distribution analysis to determine the intensities of the various transitions, as described in Sec. IIIB. The peaks are labeled according to the energies (in MeV) of the initial and final states of the nucleus between which the transitions occur. Their assignments to transitions in B¹¹ and C¹¹ are discussed in Sec. IIIC. The 3.09-, 3.68-, and 3.86-MeV lines from C¹²(d,p γ)C¹³ are also evident in the B¹⁰+d spectrum, and are so labeled. They are particularly intense because of the large amount of carbon in the B¹⁰ target. The 2.31-MeV line apparent in Fig. 5(a) arises largely from the C¹²(He³,p)N¹⁴ reaction, while the Pb²⁰⁸ 2.62 → 0 transition arises from inelastic scattering of neutrons in the lead shielding of the spectrometer.

B. Analysis

The spectra recorded at the various angles of observation were analyzed using a computer-implemented least-squares program which fits the individual lines of the spectrum with a functional form comprised of a Gaussian peak plus an exponential tail. Previous studies¹⁶ of monoenergetic transitions ranging from 2 to 7 MeV have determined the energy dependences of those parameters which define the line shape, namely, the line width σ and the "tail" parameters C and D which define the relative amplitudes and slope of the

exponential tails. These dependences are

$$\sigma = (0.5 + 2.86/\sqrt{E})E;$$

$$C = 1.0 \times 10^{-4}(E)^{3/2}; \text{ and } D = 3.4 \times 10^{-3}/\sqrt{E},$$

where

$$E = E_\gamma - 1.022.$$

In the present work, therefore, we have assumed the above dependences, and hence the only free parameters available for the computer fit are those of interest here: the peak position E_γ and peak area A_γ . The areas determined for the various angles of observation were fitted with a Legendre polynomial expansion of the form $W(\theta) = I_\gamma \sum a_\nu P_\nu(\cos\theta)$ for even values of ν with $a_0 = 1$. All of the data could be fitted with $\nu \leq 2$, as given in Table II. However, the solutions for $\nu_{\max} = 4$ are also given in Table II since it is desirable to set an upper limit on possible a_4 coefficients in order to interpret the magnetic spectrometer results.

The relative intensities were computed from the fitted angular distributions and peak areas using the efficiency factor ξ_p determined previously.¹⁶ This factor, ξ_p , expresses the energy dependence of the pair cross section, allowing for small corrections arising from the finite crystal dimensions, and includes also the empirically determined variation of peak-to-total counting rates for the pair spectrometer. The results are summarized in Table II for both the $\text{Be}^9 + \text{He}^3$ and $\text{B}^{10} + d$ reactions, which are discussed separately below. The first two columns list, respectively, the transition energies (in MeV) and the initial and final states of the nucleus to which the transitions are assigned. The experimentally determined values for the relative line intensities I_γ are given in columns 3 and 6. The coefficients a_2 obtained from the Legendre polynomial fit for $\zeta \leq 2$ are given in columns 4 and 7. In columns 5 and 8 are listed the solutions for the ratio a_4 obtained for $\zeta \leq 4$. Since in all cases the values for a_2 with $\zeta \leq 4$ match those obtained for $\zeta \leq 2$, the former are not given. Not all of the transitions listed in columns 1 and 2 are seen in both reactions, as is evident from Fig. 5 and from the intensities listed in Table II. The symbol W is used to denote lines which are indeed present, but unresolved from stronger lines, while No signifies the particular line is *not* in evidence to any measurable extent. For several of the less intense lines listed in Table II only values for I_γ are listed. For these transitions it appears that possible anisotropies are limited to $|\alpha_\nu| < 0.3$. However, the difficulties involved in determining the angular variation in intensity of such relatively weak peaks superimposed on an angle-dependent "background" (i.e., tails of higher lying lines plus a small real background) precluded a more accurate determination of the angular-distribution coefficients.

C. Results

The $\text{Be}^9(\text{He}^3, p\gamma)\text{B}^{11}$ and $\text{Be}^9(\text{He}^3, n\gamma)\text{C}^{11}$ Reactions

Figure 5(a) shows the 3-crystal pair spectrum from $\text{Be}^9 + \text{He}^3$ measured at a He^3 bombarding energy of 3.2

MeV and a detector angle of $\theta_\gamma = 90^\circ$. The solid curve through the data points is the fitted spectrum obtained through the analysis described in Sec. IIIB. The transitions labeled in Fig. 5 are those which were assumed to be present in performing the computer fit to the data.

The three higher lying transitions are assigned to B¹¹ on the basis of the proton-gamma coincidence results of Sec. II. There was no evidence for gamma-ray emission from C¹¹ levels unbound against α -particle decay. The energies of the three highest energy lines agree well with those expected for the ground-state transitions from the 8.92-, 8.57-, and 7.99-MeV levels of B¹¹. The fact that the C¹¹ 7.50 \rightarrow 0 transition is not resolved from the B¹¹ 7.30 \rightarrow 0 transition leads to the somewhat larger error limits quoted for the intensity and angular-distribution coefficients of these lines. It is evident from the breadth of the prominent peaks at 6.90 and 6.35 MeV that each results as a superposition of two or more unresolved components. Subsequent investigations utilizing the inherently better resolution of the magnetic pair spectrometer disclose the presence of a decidedly weaker B¹¹ 6.76 \rightarrow 0 component in the C¹¹ 6.90 \rightarrow 0 peak, and a weak C¹¹ 6.49 \rightarrow 0 component in the C¹¹ 6.35 \rightarrow 0 peak. This information provides assurance that the results of the analysis presented in Table II were not significantly in error due to the presence of the weaker components. The 5.86- and 5.50-MeV gamma rays are assigned to the first-excited-state decays of the B¹¹ 7.99- and C¹¹ 7.50-MeV levels. Similarly, the 5.03- and 4.81-MeV lines are assigned to the ground-state transitions of the corresponding levels in B¹¹ and C¹¹, respectively.

The computer analysis of the 3-crystal spectra gives clear evidence for the existence of a weak transition of about 4.67 MeV (6.81 \rightarrow 2.14), again in agreement with the results of the later magnetic spectrometer measurements. The peak at ~ 4.4 MeV has been resolved into two components corresponding to the B¹¹ 4.46 \rightarrow 0 and C¹¹ 4.32 \rightarrow 0 transitions. The somewhat larger errors assigned to the values quoted in Table II for I_γ and the angular-distribution coefficients of these transitions reflect the uncertainty with which the analysis succeeds in separating the two components. Similarly, the peak at ~ 2.85 MeV is resolved into two components, assigned to the B¹¹ 5.03 \rightarrow 2.14 and C¹¹ 4.81 \rightarrow 2.00 transitions.

The $\text{B}^{10}(d, p\gamma)\text{B}^{11}$ and $\text{B}^{10}(d, n\gamma)\text{C}^{11}$ Reactions

With few exceptions the transitions evident in the $\text{Be}^9 + \text{He}^3$ reaction spectrum are also evident in the $\text{B}^{10} + d$ spectrum. The present results are in agreement with those reported in studies^{20,21} of the proton spectrum from the $\text{B}^{10}(d, p)\text{B}^{11}$ reaction. These studies showed that the B¹¹ levels at 8.92 and 6.76 MeV were strongly fed, the levels at 8.57, 7.99, 7.30, 6.81, 5.03, and

²⁰ O. M. Bilaniuk and J. C. Hensel, Phys. Rev. **120**, 211 (1960).

²¹ S. Hinds and R. Middleton, Nucl. Phys. **38**, 114 (1962).

TABLE III. Branching ratios for the bound levels of B¹¹.

E_i (MeV)	E_f (MeV)	E_γ (MeV)	Branching ratios (%)					Average
			a	b	c	d	e	
4.46	0	0	100	100	100			100
	2.14	2.32	<1	<0.5	...			<0.5
5.03	0	5.03	84±2	86±3	88			85±2
	2.14	2.89	16±2	14±3	12			15±2
	4.46	0.57	...	<0.3	...			<0.3
6.76	0	6.76	72±2		83	57±3		70±2
	2.14	4.62	<3		<8	...		<3
	4.46	2.30	28±2		17	43±3		30±2
	5.03	1.73	<1			<1
6.81	0	0	65±8		79		68	71±5
	2.14	4.67	35±8		21		32	29±5
	4.46	2.35	<8		<8
	5.03	1.78	<8		<8
7.30	0	7.30	87±2		93			87±2
	2.14	5.16	<1		...			<1
	4.46	2.84	5.5±1		7			5.5±1
	5.03	2.27	7.5±1		...			7.5±1
7.99	0	7.99	47±2		55		42	47±2
	2.14	5.85	53±2		45		58	53±2
	4.46	3.53	<1		<1
	5.03	2.96	<1		<1
8.57	0	8.57	56±2		62			56±2
	2.14	6.43	30±2		28			30±2
	4.46	4.11	5±1		10			5±1
	5.03	3.54	9±1		...			9±1
8.92	0	8.92	95±1		86	95±2		95±1
	2.14	6.78	<1		9			<1
	6.76	2.16	<1		...			<1
	6.81	2.11	<1		...	2.5±1		<1
	5.03	3.89	<1		...			<1
	4.46	4.46	5±0.5		5	2.5±1		4.5±0.5

^a Present work.

^b P. F. Donovan, J. V. Kane, R. E. Pixley, and D. H. Wilkinson, Phys. Rev. **123**, 589 (1961).

^c A. J. Ferguson, H. E. Gove, J. A. Kuehner, A. E. Litherland, E. Almqvist, and D. A. Bromley, Phys. Rev. Letters **1**, 414 (1958). Errors are quoted as ±6 but are smaller for weak transitions.

^d L. L. Green, G. A. Stephens, and J. C. Willmott, Proc. Phys. Soc. (London) **79**, 1017 (1962).

^e D. H. Wilkinson and D. E. Alburger, Phys. Rev. **113**, 563 (1959). Errors not quoted.

2.14 MeV were only weakly fed, while the 4.46-MeV level was populated to some intermediate extent. The transitions from these levels are clearly evident in Fig. 5(b) and are labeled accordingly. Transitions corresponding to the decay of levels in C¹¹ at 6.49, 4.81, 4.32, and 2.00 MeV are also evident. The presence of a weak 5.50-MeV peak indicates that the C¹¹ 7.50-MeV level is being populated; however, in this case, the 7.50→0 transition is too weak to be seen in the presence of the much stronger B¹¹ 7.30→0 transition.

Branching Ratios in B¹¹ and C¹¹

These 3-crystal spectrometer studies give some further information on the branching ratios of the B¹¹ levels and also some information on the branching ratios of C¹¹ levels. In particular the following intensity ratios of transitions in B¹¹ can be obtained from the data given in Table II: (5.03→2.14)/(5.03→0), (6.76→4.46)/(6.76→0), (7.99→2.14)/(7.99→0), and (8.57→5.03)/(8.57→0). The results for these ratios are all in good agreement with the branching ratios given in Table I. For C¹¹ we obtain intensity ratios for (4.81→2.00)/(4.81→0) and (7.50→2.00)/(7.50→0). Upper limits can be extracted for several transitions; however, for B¹¹ these are not as restrictive as those obtained from the proton-gamma coincidence studies.

All our results for branching ratios in B¹¹ and C¹¹ are

collected in Tables III and IV, where our results are compared to previous work. For both B¹¹ and C¹¹ the weighted average of all the results given for each transition is also given. Since uncertainties were not always quoted in previous work the averaging procedure is somewhat arbitrary.

For B¹¹ our results in Table III are averages of the proton-gamma coincidence work (Table I) and the 3-crystal spectrometer results (Table II). The results in Table IV are from the 3-crystal spectrometer studies. In addition, both tables contain some information from the magnetic spectrometer studies described in the next section. In particular the intensity ratios (7.99→2.14)/(7.99→0) and (7.50→2.00)/(7.50→0) in B¹¹ and C¹¹, respectively, were carefully measured using the magnetic spectrometer, since the C¹¹ 7.50→0 transition was not resolved from the B¹¹ 7.30→0 transition in the 3-crystal spectrometer spectra (see Fig. 5). The result obtained for the decay of the C¹¹ 7.50-MeV level is given in Table IV. The result for the B¹¹ 7.99-MeV level decay was (57±3)% and (43±3)% for the branching ratios of the 7.99→2.14 and 7.99→0 transitions, in fair agreement with the average result given in Table III. This serves as a check on the result obtained with the magnetic spectrometer for the decay of the C¹¹ 7.50-MeV level.

In general our results are in good agreement with previous work, but there are a few instances of disagreement. In B¹¹ (Table III) the three measurements quoted for the relative intensities of the (6.76→4.46) and (6.76→0) transitions are in rather poor agreement. In this case we measured the ratio of these two transitions by two different methods and obtained good agreement between them. Also, we observed no evidence for transitions from the B¹¹ 8.92-MeV level to the 2.14-, 6.76-, or 6.81-MeV levels in contradiction to the

TABLE IV. Branching ratios for the bound levels of C¹¹.

E_i (MeV)	E_f (MeV)	E_γ (MeV)	Branching ratios (%)					Average
			a	b	c	d	e	
4.32	0	4.32		100	100			100
	2.00	2.32		<2	<3			<2
4.81	0	4.81	83±5	85±5	80±7			83±4
	2.00	2.81	17±5	15±5	20±7			17±4
6.35	0	6.35				65±3		65±3
	2.00	4.35				35±3		35±3
	4.32	2.03						<4
	4.81	1.54						<4
6.49	0	6.49		88±3		<4	89±2	89±2
	2.00	4.49		<2			<2	<2
	4.32	2.17		12±3			11±2	11±2
6.90	0	6.90	...	>80	89±3			89±3
	2.00	4.90	...	<20	<2			<2
	4.32	2.58	≤11±2	>20	11±3			11±3
	4.81	2.09	...	<20	<3			<3
7.50	0	7.50	38±2			25±5		36±2
	2.00	5.50	62±2			75±5		64±2
	4.32	3.18	<3			<5		<3
	4.81	2.69	<6			<3		<3

^a Present work.

^b P. F. Donovan, J. V. Kane, R. E. Pixley, and D. H. Wilkinson, Phys. Rev. **123**, 589 (1961).

^c R. M. Freeman, Nucl. Phys. **37**, 215 (1962).

^d M. L. Roush, A. A. Jaffe, A. S. Figueroa, and W. F. Hornyak, Bull. Am. Phys. Soc. **9**, 55 (1964); Nucl. Phys. (to be published).

^e D. W. Braben, P. J. Riley, and G. C. Neilson, Can J. Phys. **41**, 784 (1963).

results of Ferguson, *et al.*⁶ and Green, Stephens, and Willmott.³ In C¹¹ the only discrepancy is in the intensity ratio (7.50 → 2.00)/(7.50 → 0). In this case we obtained (46±5)% and (36±2)% for the 7.50 → 0 branch from the 3-crystal spectra (Table II) and the magnetic spectrometer results, respectively. The average is (38±2)%. This is to be compared to the only previous result²² of (25±5)%.

Lifetime Limits for the Bound Levels of B¹¹ and C¹¹

The relative energies of most of the gamma-ray lines observed in 3-crystal pair spectra such as those of Fig. 5 can be determined to better than 10 keV by computer analysis if a careful calibration of pulse height versus energy is made. In the present work such a calibration was not made and a small nonlinearity in the response of the detection system introduced uncertainties of about 0.5% into the energy measurements. Nevertheless it was still possible to study the variation of energy of a given gamma-ray line as a function of the angle of detection since in this case the nonlinearity drops out to first order. Such a study was made in the present work in order to gain information on the lifetimes of the bound states of B¹¹ and C¹¹ from determinations of the Doppler shifts of the various transitions.

The method used was to adopt the B¹¹ 8.92 → 0 transition as an energy standard and to calculate the energies of the other transitions relative to it for all five angles of observation. All transitions were assumed to have an energy dependence on the angle of detection (θ) given by

$$E_\gamma(\theta) = E_\gamma(90^\circ) + \Delta E_{\text{expt}} P_1(\cos\theta), \quad (1)$$

where $P_1(\cos\theta)$ is the first Legendre polynomial ($\equiv \cos\theta$), and ΔE_{expt} is the Doppler shift which is a function of the kinematics of the reaction (including the unknown angular distribution of the reaction products) and the lifetime of the emitting level. For the B¹¹ 8.92 → 0 transition ΔE_{expt} was taken to be 96 and 70 keV for the Be⁹+He³ and B¹⁰+d reactions, respectively. These values are those calculated for the kinematics of the respective reactions with the outgoing protons assumed to have an average center-of-mass angle of 70° to the beam axis in both cases. The assumed value for the average center-of-mass reaction angle is somewhat arbitrary; its justification lies partially in the consistency of the final results and partially in past experience which indicates that reactions of the type involved here almost always have angular distributions which correspond to average reaction angles in the range 50°–90°.

The 8.92 → 0 transition was chosen as the energy standard not only because it was the most energetic transition observed, but also because the 8.92-MeV level is known from the Li⁷(α,γ)B¹¹ results^{3,18} to have a

²² M. L. Roush, A. A. Jaffe, A. S. Figuera, and W. F. Hornyak, Bull. Am. Phys. Soc. 9, 55 (1964); Nucl. Phys. (to be published).

TABLE V. Doppler shift (0°–90°) measurements for gamma rays from B¹¹ and C¹¹.

E_γ (MeV)	E_i (MeV)	Be ⁹ +He ³		B ¹⁰ +d	
		ΔE_{expt} (keV)	F'	ΔE_{expt} (keV)	F'
8.92	B ¹¹ 8.92	(96)	(1.000)	(70)	(1.000)
8.57	B ¹¹ 8.57	83±15	1.02±0.18		
7.99	B ¹¹ 7.99	79±15	0.93±0.17		
7.50	C ¹¹ 7.50	62±21	0.79±0.27		
7.30	B ¹¹ 7.30	63±13	0.82±0.17	60±7	1.10±0.14
6.90	C ¹¹ 6.90	63±7	0.88±0.09		
6.76	B ¹¹ 6.76			51±7	1.01±0.14
6.49	C ¹¹ 6.49			50±6	1.05±0.12
6.35	C ¹¹ 6.35	66±7	1.00±0.10		
5.86	B ¹¹ 7.99	63±9	1.05±0.16		
5.50	C ¹¹ 7.50	62±7	1.11±0.12		
5.03	B ¹¹ 5.03	52±6	1.02±0.12	45±8	1.27±0.22
4.81	C ¹¹ 4.81	47±8	0.98±0.17	32±5	0.95±0.15
4.46	B ¹¹ 4.46	49±10	1.15±0.23	37±4	1.18±0.12
4.32	C ¹¹ 4.32	45±7	1.05±0.16	35±5	1.20±0.18
3.54	B ¹¹ 8.57	54±13	1.55±0.37		
2.93	B ¹¹ 5.03	54±17	1.91±0.59		
2.83	C ¹¹ 4.81	36±13	1.27±0.45		
2.30	B ¹¹ 6.76	32±7	1.42±0.33		
2.14	B ¹¹ 2.14	26±3	1.17±0.11		
2.00	C ¹¹ 2.00	24±3	1.17±0.13		
3.86	C ¹³ 3.85			8±4	0.30±0.16
3.68	C ¹³ 3.68			18±4	0.70±0.16
3.09	C ¹³ 3.09			22±2	1.06±0.08

lifetime very short compared to the stopping time of nuclei in solids.

The energies of the various gamma-ray lines were determined at each of the five angles with the energy calibration fixed by the position of the 8.92-MeV line and an assumed linear relationship between energy and pulse height. The uncertainties assigned to the energy values were those generated by the computer fits to the pair spectra. A least-squares fit was made to Eq. 1 for each of the lines. The results obtained for ΔE_{expt} are listed in Table V. The uncertainties assigned to the ΔE_{expt} are those determined by the computer fit to Eq. (1).

From inspection of Table V it can be seen that all the bound levels of B¹¹ and C¹¹ (save the B¹¹ 6.81-MeV level for which no information was obtained) decay by one or more transitions with nonzero Doppler shifts. Thus all these levels have lifetimes shorter than, or comparable to, the stopping time of B¹¹ and C¹¹ nuclei in the targets used.

In order to set lifetime limits on the bound states of B¹¹ and C¹¹ from these results we estimate the expected Doppler shifts for very short lifetimes in the same manner as we did for the 8.92 → 0 transition; that is, from the kinematics of the reaction assuming a mean value of 70° for the reaction angle of the outgoing nucleon. This method is not correct for transitions which originate from excited states fed by gamma-ray cascades from higher states; however, the uncertainty from this source of error is, for our purposes, small enough to be ignored. The measured ΔE_{expt} were divided by the calculated ΔE to produce an estimate of the

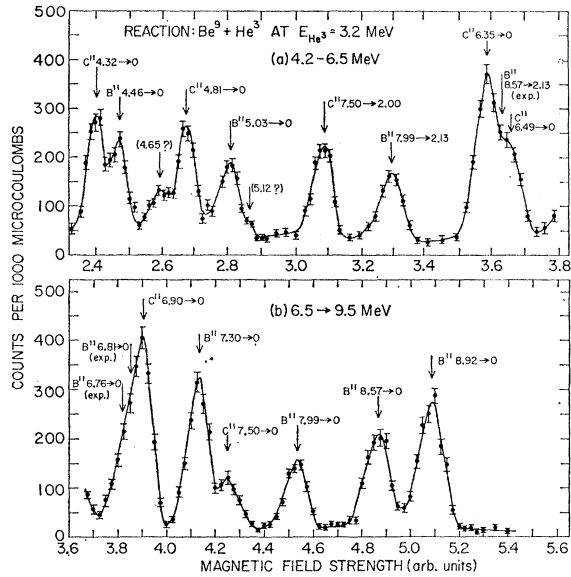


FIG. 6. Spectrum of internal pairs from levels of B^{11} and C^{11} populated in the $Be^9(He^3,p)B^{11}$ and $Be^9(He^3,n)C^{11}$ reactions. The data were recorded at a He^3 bombarding energy of 3.2 MeV with the intermediate-image spectrometer operating at a resolution setting of 1.95%. The various peaks are identified by the energies (in MeV) of the initial and final levels of the nucleus between which the transitions occur. The calculated expected positions of some unresolved lines are indicated by (exp). With the better resolution of the intermediate-image spectrometer (as compared to that obtained with the 3-crystal pair spectrometer as illustrated in Fig. 5) the presence of the $B^{11} 6.81 \rightarrow 2.14$ transition and the $C^{11} 6.49 \rightarrow 0$ transition is readily apparent, as is also the 5.10-MeV contaminant peak due to the $C^{12}(He^3,p)N^{14}$ reaction. Note that only an approximate normalization is obtained for the data plotted in (a) and (b), since the measurements were made using two different Be^9 targets.

Doppler shift attenuation factor F' , which is unity for very short lifetimes and 0 for very long lifetimes.²³

The values of F' listed in Table V have a mean value near unity and a distribution about the mean which is consistent with the assigned errors (11 out of 28 fall further than one standard deviation from unity) assuming all the levels have very short lifetimes. The only transition with an F' value strongly inconsistent with unity is the $C^{13} 3.85 \rightarrow 0$ transition and the $C^{13} 3.85$ -MeV level is known²⁴ to have a lifetime comparable to the stopping time of the C^{13} recoils.

To simplify the analysis of these data we adopt the single limit $F' > 0.5$ for all the measured transitions of B^{11} and C^{11} . We then use the simplified expression²³

$$F' = (\alpha/\tau)/(1 + \alpha/\tau), \quad (2)$$

where α is the stopping time of the B^{11} or C^{11} nuclei in the targets (Be^9 or a mixture of B^{11} powder and carbon) and τ is the mean lifetime of the excited state in question. The stopping time α is about 5×10^{-13} sec for both

B^{11} and C^{11} stopping in either target²³ so that the limit $F' > 0.5$ corresponds roughly to $\tau < 5 \times 10^{-13}$ sec. This then is the limit we adopt for all the bound levels of B^{11} and C^{11} save the $B^{11} 6.81$ -MeV level.

IV. INTERNAL PAIR MEASUREMENTS

A. The Spectra of Internal Pairs

The spectra of internal pairs emitted from B^{11} and C^{11} were studied using the Brookhaven magnetic-lens intermediate-image spectrometer.²⁵⁻²⁷ The spectra were quite similar to those obtained with the 3-crystal pair spectrometer since the dependence on transition energy of internal pair production is quite similar to that of external pair production. The important difference is that the resolution obtained with the magnetic spectrometer was varied between 1.6% and 3% full width at half-maximum (FWHM) as opposed to a fixed value of about 4% for the 3-crystal pair spectra.

The spectrum of internal pair lines from $Be^9 + He^3$ at a bombarding energy of 3.2 MeV is shown in Fig. 6. In Fig. 6, as opposed to Fig. 5(a), the $C^{11} 7.50 \rightarrow 0$ transition is resolved from the $B^{11} 7.30 \rightarrow 0$ transition. Similar spectra were used to measure the intensity ratio $(7.50 \rightarrow 2.00)/(7.50 \rightarrow 0)$ as explained in Sec. IIIC.

The branching ratios presented in Tables III and IV were a great aid in disentangling the pair spectra. For example the known branching ratios of the $B^{11} 6.81$ -MeV level together with the measured intensity of the $B^{11} 6.81 \rightarrow 2.14$ transition allowed an estimate of the contribution of the $B^{11} 6.81 \rightarrow 0$ transition to the unresolved triplet of which the $C^{11} 6.90 \rightarrow 0$ transition is the most prominent member. Similarly, the contribution of the $B^{11} 8.57 \rightarrow 2.14$ transition to the unresolved triplet dominated by the $C^{11} 6.35 \rightarrow 0$ transition was obtained.

The transition labeled $N^{14} 5.10 \rightarrow 0$ in Fig. 6 arises from the $C^{12}(He^3,p\gamma)N^{14}$ reaction as does the $N^{14} 2.31 \rightarrow 0$ transition [Fig. 5(a)]. The contribution of other N^{14} transitions from this contaminant reaction could be estimated from the intensities of these two pair lines using results from previous work¹⁶ on the $C^{12}(He^3,p)N^{14}$ reaction.

A partial internal pair spectrum from $B^{10} + d$ at 3.0-MeV bombarding energy is shown in Fig. 7. This spectrum was recorded at a resolution of 1.65% (FWHM), and shows more clearly the contribution of various transitions to the doublet labeled $C^{11} 6.49 \rightarrow 0$, $B^{11} 6.76 \rightarrow 0$ in Fig. 5(b). From spectra of this type together with the results presented in Secs. II and III it was possible to estimate quite accurately the relative contributions of all the possible B^{11} and C^{11} transitions to unresolved pair lines. This was critical to the interpretation of the internal pair correlation measurements reported in the next subsection.

²³ E. K. Warburton, D. E. Alburger, and D. H. Wilkinson, Phys. Rev. **129**, 2180 (1963).

²⁴ J. J. Simpson, M. A. Clark, and A. E. Litherland, Can. J. Phys. **40**, 769 (1962).

²⁵ D. E. Alburger, Rev. Sci. Instr. **27**, 991 (1956).

²⁶ D. E. Alburger, Phys. Rev. **111**, 1586 (1958).

²⁷ D. E. Alburger, Phys. Rev. **118**, 235 (1960).

B. Internal Pair Correlation Measurements

Theory

The utilization of the intermediate-image spectrometer for determining the multipolarity of electromagnetic transitions between nuclear states has been described in some detail previously.^{15,16} We wish here to consider additional theoretical calculations which were employed in the interpretation of the present experiments.

To recapitulate: Positron-electron pairs emitted from the source region at a mean angle α with respect to the spectrometer axis are focused by the axial magnetic field of the spectrometer to a finite-size image at the opposite image position, where they are detected in two opposed hemi-cylindrical detectors operated in coincidence. By means of a spiral baffle located just after the annulus at the intermediate image, the positrons and electrons are limited to different ranges of azimuthal angles as determined by the respective sector angles ω_+ and ω_- . Referring to the *emission* plane, this corresponds to restricting the positrons to the range of azimuthal angles ϕ_+ given by $-\omega/2 \leq \phi_+ \leq \omega/2$ and correspondingly for electrons $\pi - \omega/2 \leq \phi_- \leq \pi + \omega/2$. Removing the baffle has been shown to be equivalent to letting $\omega/2 \rightarrow \pi/2$. By measuring, for a given pair line, the *net* coincidence counts with baffle in (Y_{in}) and the *net* coincidence counts with baffle out (Y_{out}) one determines the experimental ratio $R_\omega' = Y_{in}/Y_{out}$. The relationship between R_ω' and the multipolarity of the transition has been given previously for the case where the *mean* azimuthal angles $\bar{\phi}_+$ and $\bar{\phi}_-$ are, as indicated above, different by exactly π , i.e., $(\bar{\phi}_- - \bar{\phi}_+) = \pi$. We here indicate the extension of this calculation to the case $(\bar{\phi}_- - \bar{\phi}_+) = \pi + \Delta$ where Δ expresses the deviation from precise symmetry in the *emission* plane.

The necessary relationships and notations are given in Eqs. (1) through (10) of the previous presentation.¹⁵ Briefly, the dependence of the theoretical ratios R_ω' upon the spectrometer geometry is contained in the function $I_n(\omega, \alpha) = [(1/2\pi)(\sin^{2n-4}\alpha)]J_n(\omega)$. Since the expression in square brackets depends only on the emission angle α , it is sufficient here to examine the changes wrought in $J_n(\omega)$ by the inclusion of the term Δ to give the function $J_n(\omega, \Delta)$. Referring to Eq. (8) of Ref. 15 and using the limits of integration on ϕ_+ and ϕ_- implied above, the general expression for $J_n(\omega, \Delta)$ becomes

$$J_n(\omega, \Delta) = \frac{1}{2\pi} \int_{-\omega'/2}^{\omega''/2} d\varphi_+ \int_{\pi-\varphi_+-\omega''/2}^{\pi-\varphi_++\omega'/2} \frac{\sin^{2n}(\varphi/2) d\varphi}{[d^{-1} + \sin^2(\varphi/2)]^2}. \quad (3)$$

For brevity, it is convenient to define the quantity

$$X(\omega, \Delta) \equiv \int_{\tan(\Delta/2)}^{\tan(\omega'/2)} \frac{\tan^{-1}(ay) dy}{1+y^2} + \frac{1}{2} \int_{\tan(\omega'/2)}^{\tan(\omega''/2)} \frac{\tan^{-1}(ay) dy}{1+y^2}. \quad (4)$$

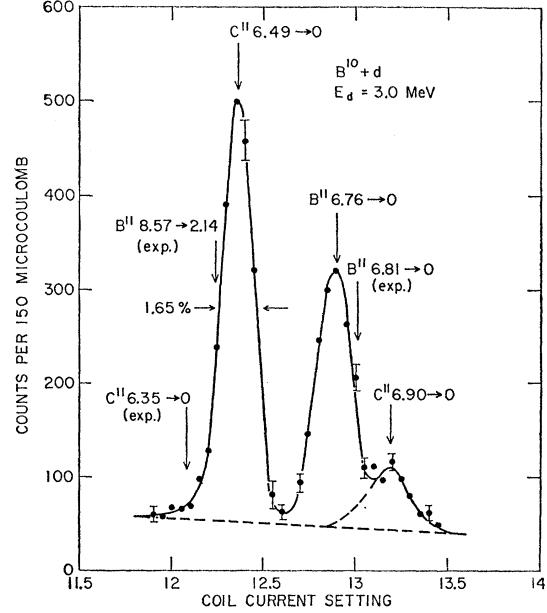


FIG. 7. Partial spectrum of internal pair lines from levels of B¹¹ and C¹¹ populated by 3.0-MeV deuteron bombardment of a B¹⁰ target, indicating possible contributions from other lines to the C¹¹ 6.49 \rightarrow 0, B¹¹ 6.76 \rightarrow doublet. Data such as these were used to estimate the possible influence of weaker unresolved lines on the values of R_ω measured for the various stronger lines of the spectrum.

The solutions for $J_n(\omega, \Delta)$ are then given as

$$J_0(\omega, \Delta) = \frac{2}{\pi^2} J_0(2\pi) X(\omega, \Delta) - \frac{d^2}{\pi(d+1)} \times \ln \left\{ \frac{g + \cos \Delta}{[(g + \cos \omega')(g + \cos \omega'')]^{1/2}} \right\} \quad (5)$$

$$J_1(\omega, \Delta) = \frac{2}{\pi^2} J_1(2\pi) X(\omega, \Delta) + \frac{d}{\pi(d+1)} \times \ln \left\{ \frac{g + \cos \Delta}{[(g + \cos \omega')(g + \cos \omega'')]^{1/2}} \right\}, \quad (6)$$

and the recurrence formula for $n \geq 2$,

$$J_n(\omega, \Delta) = \frac{1}{2\pi} \int_{-\omega'/2}^{\omega''/2} d\varphi_+ \int_{\varphi_+-\omega''/2}^{\varphi_++\omega'/2} \cos^{2n-4}(\varphi/2) d\varphi - (2/d)J_{n-1}(\omega, \Delta) - (1/d^2)J_{n-2}(\omega, \Delta). \quad (7)$$

In the above equations we have defined $\omega' \equiv \omega - \Delta$, $\omega'' \equiv \omega + \Delta$, and $g \equiv (2+d)/d$. The other quantities have been defined previously.¹⁵ Note that for $\Delta \rightarrow 0$ the second integral of Eq. (4) also goes to zero, and we have remaining the term given previously for the case of symmetric emission sectors. Similarly, for $\Delta = 0$, $\omega' = \omega'' = \omega$, and Eqs. (5) through (7) reduce to those given previously for $J_n(\omega)$.

It was previously asserted¹⁵ that the effect of making $\Delta > 0$ could be simulated by assuming a value for ω

TABLE VI. Summary of experimental calibration ratios R_{ω}' and the corrected ratios R_{ω} obtained in the present work and the R_{ω} obtained with previous baffle systems (Refs. 15 and 16).

Transition	Multipolarity	R_{ω}' (present work)	R_{ω} (present work)	R_{ω} (Ref. 15)	R_{ω} (Ref. 16)
C ¹³ 3.09 → 0	E1	0.179±0.005	0.179±0.005	0.185±0.008	0.178±0.006
Be ¹⁰ 3.37 → 0	E2	0.129±0.003	0.126±0.004	0.130±0.004	0.130±0.004
Li ⁶ 3.56 → 0	M1	0.093±0.003	0.093±0.003	0.092±0.002	0.104±0.003
C ¹³ 3.85 → 0	M2	0.057±0.002	0.056±0.003	0.056±0.005	0.063±0.003
C ¹² 4.43 → 0	E2			0.097±0.005	0.097±0.003
Be ¹⁰ 5.96 → 0	E1	0.098±0.003	0.098±0.003	0.102±0.003	0.112±0.002
O ¹⁶ 6.06 → 0	E0	0.256±0.003	0.267±0.005	0.265±0.005	0.264±0.003
N ¹⁴ 6.44 → 0	E2	0.080±0.004	0.068±0.004		0.082±0.006
N ¹⁵ 8.31 → 0	E1	0.071±0.002	0.071±0.002		

somewhat larger than the measured geometric sector angle. Calculations made using the above equations serve to verify this assertion. The principal advantage to be gained from including Δ explicitly in the calculations is that it *reduces* the number of free parameters available for fitting the experimental calibration data, since α , ω , Δ are all geometrical constants which have been measured and can be constrained to assume only those values allowed by the uncertainties in their measurements. The only remaining parameter needed to represent the theoretical R_{ω}' is the normalization factor $C(\omega)$ which expresses the variation in experimental efficiencies for the Y_{in} and Y_{out} measurements,¹⁵ and this parameter, which is essentially geometrical, is also constrained to vary within the limits allowed by the experimental uncertainties in its measurements.

For the present baffle system we find from geometrical measurements: $\omega = (108 \pm 2)^\circ$, $\alpha = (45.7 \pm 1)^\circ$ and $\Delta = (26 \pm 10)^\circ$. The efficiency ratio $C(\omega)$, is determined from the ratio of solid angles with and without baffle and from the ratio of singles counting rates with and without baffle. We find $C(\omega) = 3.75 \pm 0.20$.

Calibration Measurements

In order to calibrate the spectrometer for further studies of nuclear transitions of unknown multipolarity, we have remeasured experimental ratios R_{ω}' for a number of transitions whose multiplicities are known. The general procedure has been described previously.¹⁵ The results are given in Table VI. The N¹⁵ 8.31 → 0 transition, not included in previous measurements, was formed by the N¹⁴(*d,p*)N¹⁵ reaction at a bombarding energy of 3 MeV.

The first column in Table VI gives the nucleus and the energies (in MeV) of the initial and final states between which the transition occurs. The character of the radiation is designated in the next column. The experimentally measured values of R_{ω}' (direct) and R_{ω} (after alignment corrections)¹⁵ are given in columns 3 and 4.

Values of R_{ω} measured previously under somewhat different experimental conditions are given in columns 5 and 6. A consideration of these results, in chronological order, serves to elucidate a problem which arose in the

intermediate measurements of Ref. 16. The original spiral baffle used for the measurements of Ref. 15 employed adequately large baffle blades in a rigid structure which was then moved in and out of position for the ratio measurements. The agreement between measured ratios and calculated ratios was found to be quite good with this system. However, the procedure for changing the baffle position was quite inefficient; accordingly, a new baffle system was installed which could be much more readily moved to the baffle-in and baffle-out positions. However, it was noted that the ratios R_{ω}' measured for the calibration lines were systematically larger than the values measured previously, the effect being greatest for large transition energy and/or small R_{ω}' . This may be seen from the results given in columns 5 and 6 of Table VI.

An investigation of this feature, which prompted the additional calculations described here, led to the conclusion that the observed deviation did not arise from a changed geometry, since α , ω , Δ were essentially the same for the two baffle systems. However, it was noted that the effect could be produced by a small "leak through", i.e., the baffle was not 100% efficient in stopping particles of the wrong sign. It was subsequently noted that the new baffle blades were indeed smaller than those of the original rigid baffle. Accordingly, the blade size was increased to correspond to the size obtained for the original baffle, and the calibration measurements were repeated. The results are found to agree with those obtained previously in Ref. 15 and indicate little, if any, "leak through".

The value of R_{ω} given for the O¹⁶ 6.06-MeV E0 line in Table VI is about 4% higher than the measured value, R_{ω}' . This increase was made in an attempt to compensate approximately for such processes as scattering of electrons (and positrons) in the target, target holder, baffle system, annulus, etc., and an expected small dependence of $C(\omega)$ on $R_{\omega}(l)$. These effects and several others which are expected but which are not incorporated in the theoretical calculations all tend to decrease the separation between the $R_{\omega}(l)$ for different l (multipolarity) and can be partially accounted for by raising $R_{\omega}(E0)$ since it is separated appreciably from the other $R_{\omega}(l)$. The 4% by which the experimental

value for $R_\omega(E0)$ was raised is our estimate of the accumulated effect of these processes on the separation of $R(E0)$ from $R(E1)$ for 6-MeV transitions.

The results of the present calibration measurements are shown by the open circles of Fig. 8. The solid curves are those calculated from Eqs. (3) through (7) with $\alpha=44^\circ$, $\omega=108^\circ$, $\Delta=31^\circ$, and $C(\omega)=3.78$. The values of these parameters are all within the experimental uncertainties of their measurements except for α which was measured geometrically to be $(45.7\pm 1)^\circ$. The spectrometer accepts positrons (and electrons) falling within a range defined by $\alpha\pm\Delta\alpha$. For the maximum transmission—at which almost all measurements of R_ω' have been made— $\Delta\alpha$ is 6° . Since the coincidence efficiency of the spectrometer rises rapidly with decreasing α , the effective value of α will be somewhat smaller than the geometric mean; about 1 or 2 deg smaller for $\Delta\alpha=6^\circ$. For this reason we took $\alpha=44^\circ$ instead of 45.7° .

The procedure used to fit the theoretical curves for $R_\omega(l)$ to the calibration points (Table VI) was to fix α and ω at 44° and 108° , respectively, and to vary Δ and $C(\omega)$ for the best fit with both constrained within the measured values, i.e., $\Delta=26\pm 10^\circ$, $C(\omega)=3.75\pm 0.20$.

A good fit, which is shown in Fig. 8 was obtained for $\Delta=31^\circ$ and $C(\omega)=3.78$.

Measurements of R_ω' for Transitions in B¹¹ and C¹¹

The solid points with error flags shown in Fig. 8 are the R_ω measured for transitions in B¹¹ and C¹¹. The measured values are also listed in Table VII. These measurements were made with either the Be⁹+He³ reactions or the B¹⁰+d reactions using the same conditions as were used in making the 3-crystal pair spectrometer measurements. In all cases the alignment correction¹⁵ was negligible but introduced a further source of error into the R_ω extracted from the R_ω' .

As in previous work^{15,16} the identification of E1 transitions is straightforward and unambiguous. Seven E1 transitions were observed. Also, as discussed in the next

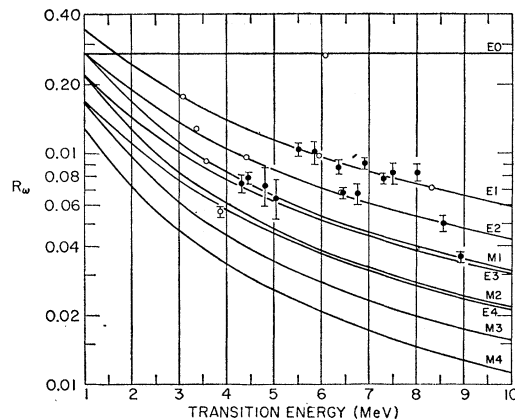


FIG. 8. Experimentally measured ratios R_ω plotted as functions of internal pair transition energies. The open circles present the results of calibration measurements for transitions of known multipolarity, as summarized in Table VI, while the curves show the theoretical values calculated for transitions of multipole order ranging from E0 to M4 and normalized as explained in the text. The results of the present measurements for transitions in B¹¹ and C¹¹, as summarized in Table VII, are shown by the solid circles. The designation of seven of these transitions as being E1 in character is readily suggested by the correspondence between the measured values and the calculated E1 curve.

section, the identification of the B¹¹ 8.92 \rightarrow 0 transition as M1 is unambiguous when the present results are combined with previous work.³

The remaining seven transitions could be M1,E2 mixtures or E1,M2 mixtures from present evidence alone; and the four lowest energy transitions shown in Fig. 8 could also be E3 or a mixture of M2 or E3.

These transitions will all be discussed in Sec. V. The most likely multipolarity for the fifteen transitions as concluded in that section are listed in the third column of Table VII. In the fourth column is listed the maximum intensity ratio, x^2 , of quadrupole radiation in the predominantly dipole transitions and M1 radiation in the predominantly E2 transitions. These limits on x^2 correspond to one standard deviation from the measured values of R_ω . The procedure for obtaining these limits has been described previously.¹⁵

V. DISCUSSION

A. Synthesis with Previous Results

Our final conclusions regarding the gamma-ray decay schemes and spin-parity assignments of the bound levels of B¹¹ and C¹¹ are collected in Figs. 9 and 10. The gamma-ray branching ratios are taken from Tables III and IV. The spin-parity assignments are obtained by combining previous work (Fig. 1) with the evidence presented in this paper, the interpretation of which we shall now discuss level by level.

The B¹¹ 9.19-MeV Level

The information that we obtained on the $J^\pi=7/2^+$, B¹¹ 9.19-MeV level was that $\Gamma_\gamma/\Gamma=0.1_{-0.05}^{+0.2}$. Values

TABLE VII. Summary of the experimental ratios R_ω for transitions in B¹¹ and C¹¹.

Transition	R_ω	Multipolarity	$x^2(\max)$
C ¹¹ 4.32 \rightarrow 0	0.074 \pm 0.007	M1	1
B ¹¹ 4.46 \rightarrow 0	0.079 \pm 0.005	M1	2
C ¹¹ 4.81 \rightarrow 0	0.073 \pm 0.014	M1,E2	...
B ¹¹ 5.03 \rightarrow 0	0.064 \pm 0.012	M1,E2	...
C ¹¹ 7.50 \rightarrow 2.00	0.104 \pm 0.007	E1	0.3
B ¹¹ 7.99 \rightarrow 2.14	0.101 \pm 0.010	E1	0.4
C ¹¹ 6.35 \rightarrow 0	0.088 \pm 0.006	E1	0.4
C ¹¹ 6.49 \rightarrow 0	0.068 \pm 0.004	E2	0.2
B ¹¹ 6.76 \rightarrow 0	0.067 \pm 0.007	E2	0.4
C ¹¹ 6.90 \rightarrow 0	0.091 \pm 0.005	E1	0.1
B ¹¹ 7.30 \rightarrow 0	0.078 \pm 0.004	E1	0.3
C ¹¹ 7.50 \rightarrow 0	0.083 \pm 0.009	E1	0.4
B ¹¹ 7.99 \rightarrow 0	0.083 \pm 0.007	E1	0.2
B ¹¹ 8.57 \rightarrow 0	0.050 \pm 0.004	E2	2
B ¹¹ 8.92 \rightarrow 0	0.036 \pm 0.002	M1	0.7

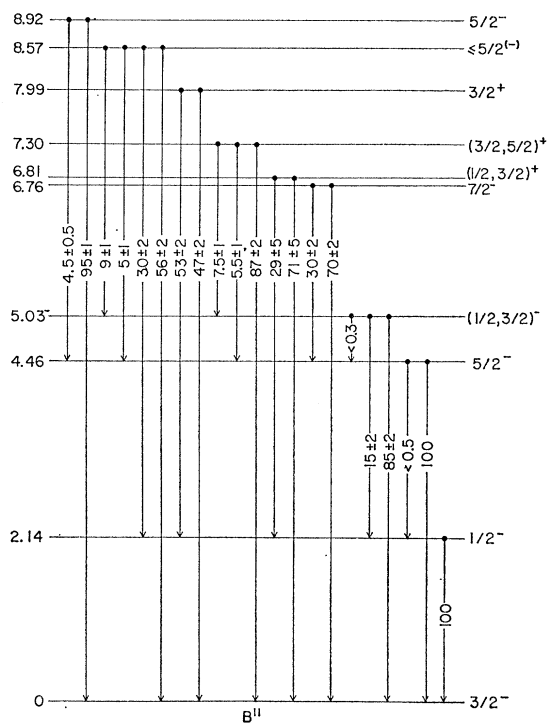


FIG. 9. Level scheme of B^{11} showing spins, parities and decay modes of those levels studied in the present experiment. The various assignments and branching ratios are obtained as a synthesis of the results of this experiment with those reported from other sources, as explained in the text. Uncertain or less likely assignments are enclosed in parentheses.

of $\Gamma_\gamma \Gamma_\alpha / \Gamma$ have been obtained for this level by means of the $Li^7(\alpha, \gamma)B^{11}$ reactions.^{3,18,28} Averaging the three values gives $\Gamma_\gamma \Gamma_\alpha / \Gamma = 0.275$ eV. Combining this with our measurement of Γ_γ / Γ gives,

$$\begin{aligned} \Gamma_\alpha &= 2.8_{-1.8}^{+2.8} \text{ eV}, \\ \Gamma_\gamma &= 0.3_{-0.01}^{+0.1} \text{ eV}; \quad \tau_\gamma = (2.2_{-0.6}^{+0.06}) \times 10^{-15} \text{ sec}, \\ \Gamma &\cong 3 \text{ eV}. \end{aligned}$$

The 9.19-MeV level is reported to have a ground-state branch of 0.9% so that $\Gamma_\gamma(\text{g.s.}) = 0.3 \times 10^{-2}$ eV.

From resonant absorption of gamma rays in B^{11} , Meyer-Schützmeister and Hanna²⁹ found $\Gamma \leq 100$ eV and $(2J+1)\Gamma_\gamma(\text{g.s.}) = 0.8$ eV for the B^{11} 9.19-MeV level. Their limit on the total width is in agreement with the present results but their value for $(2J+1)\Gamma_\gamma(\text{g.s.})$ disagrees with the value given above by a factor of about 30. Note that a radiative width of 0.1 eV for a $\frac{7}{2}^+ \rightarrow \frac{3}{2}^-$ $M2$ transition would correspond to about 20 Weisskopf units³⁰ which seems prohibitively large.

Combining a radiative width of 0.3 eV for the

B^{11} 9.19-MeV level with the branching ratios³ of 83% and 13% for the $9.19 \rightarrow 4.46$ and $9.19 \rightarrow 6.76$ transitions, respectively, gives $E1$ transition strengths of about 0.7×10^{-3} Weisskopf units for both. These seem quite reasonable. The $9.19 \rightarrow 0$ transition is reported³ to be 45% $E3$ and 55% $M2$. If so, the ground state radiative width of $(0.27 \pm 0.09) \times 10^{-2}$ eV, which is obtained from $\Gamma_\gamma = 0.3$ eV and a ground-state branching ratio³ of $(0.9 \pm 0.3)\%$, corresponds to $M2$ and $E3$ strengths of (0.3 ± 0.1) and (78 ± 26) Weisskopf units, respectively. The latter is indeed quite large. It may be that the intensity and angular-distribution measurements³ for the very weak $9.19 \rightarrow 0$ transition are liable to an uncertainty from the summing of cascade transitions. Note that the difficulty in explaining this large $E3$ strength is independent of the present measurement of Γ_γ / Γ .

The 9.19-MeV level is reported³ to be formed by the capture of f -wave α particles in the $Li^7(\alpha, \gamma)B^{11}$ reaction. A value of 2.8 eV for Γ_α corresponds to about 4% of the Wigner limit for a reaction radius of 5×10^{-13} cm. This seems a reasonable figure.

The B^{11} 8.92-MeV Level

From a study of the $Li^7(\alpha, \gamma)B^{11}$ reaction, Green, Stephens, and Willmott³ found that the B^{11} 8.92-MeV level has $J^\pi = \frac{3}{2}^+, \frac{5}{2}^+, \text{ or } \frac{5}{2}^-$ with the $8.92 \rightarrow 0$ transition 96% $E1$ plus 4% $M2$ or pure $M2$ for the $\frac{3}{2}^+$ assignment, 98% $E1$ plus 2% $M2$ or pure $M2$ for the $\frac{5}{2}^+$ assignment, and $M1$ with a 0.6% $E2$ admixture for the $\frac{5}{2}^-$ assignment. Our ratio measurement of this transition clearly rules out the $\frac{3}{2}^+$ and $\frac{5}{2}^+$ alternatives but is in good agreement with the $J^\pi = \frac{5}{2}^-$ alternative (see Fig. 8 and Table VII) which we therefore adopt for the B^{11} 8.92-MeV level.

With the B^{11} 8.92-MeV level established as $\frac{5}{2}^-$ the discrepancy between the $B^{10}(d, p)B^{11}$ stripping results of Hinds and Middleton²¹ and of Pullen and Whitehead²¹ and the $Be^9(He^3, p)B^{11}$ double stripping results of Hinds and Middleton³² on the one hand and the $B^{10}(d, p)B^{11}$ stripping results of Bilaniuk and Hensel²⁰ on the other is resolved in favor of the former measurements which indicate odd parity for the B^{11} 8.92-MeV level.

We obtained a lower limit of 0.84 (two standard deviations) for Γ_γ / Γ for the 8.92-MeV level. This limit can be combined with measured values of $\Gamma_\gamma \Gamma_\alpha / \Gamma$ for this level to give a value for Γ_α and lower limits for Γ_γ and $\Gamma = \Gamma_\alpha + \Gamma_\gamma$. The reported values of $(2J+1) \times \Gamma_\gamma \Gamma_\alpha / \Gamma$ obtained via the $Li^7(\alpha, \gamma)B^{11}$ reaction are 0.16,²⁸ 0.1,¹⁸ and 0.18³ eV. There is also a reported value of 0.036 eV,³³ which we reject as inconsistent with the

²⁸ W. F. Bennett, P. A. Roys, and B. J. Toppel, Phys. Rev. **82**, 20 (1951).

²⁹ L. Meyer-Schützmeister and S. S. Hanna, Bull. Am. Phys. Soc. **3**, 188 (1958).

³⁰ D. H. Wilkinson, in *Nuclear Spectroscopy*, edited by F. Ajzenberg-Selove (Academic Press Inc., New York, 1960) Part B, p. 852 ff.

³¹ D. J. Pullen and A. B. Whitehead, *Proceedings of the International Conference on Nuclear Structure, 1960*, edited by D. A. Bromley and E. W. Vogt (University of Toronto Press, Toronto, 1960), p. 40.

³² S. Hinds and R. Middleton, Proc. Phys. Soc. (London) **75**, 754 (1960).

³³ H. Warhanek, Phil. Mag. **2**, 1085 (1957).

other three. The average of the three measurements is 0.15 eV, and taking $J = \frac{5}{2}$ gives $\Gamma_\gamma \Gamma_\alpha / \Gamma = 0.025$ eV. Combining this value with our limit $\Gamma_\gamma / \Gamma > 0.84$ gives,

$$\begin{aligned} 0.025 \text{ eV} &\leq \Gamma_\alpha \leq 0.03 \text{ eV} \\ \Gamma_\gamma &\geq 0.15 \text{ eV}, \quad \tau_\gamma \leq 4.4 \times 10^{-15} \text{ sec} \\ \Gamma &\geq 0.18 \text{ eV}. \end{aligned}$$

According to Jones *et al.*,¹⁸ the α -particle width represents the reasonable figure of about 3% of the Wigner limit for d -wave α particles. The lower limit on the radiative width corresponds to lower limits on the $M1$ transition rates of 0.95×10^{-2} and 0.4×10^{-2} Weisskopf units for the $8.92 \rightarrow 0$ and $8.92 \rightarrow 4.46$ transitions, respectively, and 1.3×10^{-2} Weisskopf units for the $E2$ component in the $8.92 \rightarrow 0$ transition, taken to be 0.6% $E2$.³ These limits on the transition rates are considerably lower than the average speeds in light nuclei which are about 0.15 and 5 Weisskopf units for $M1$ and $E2$, respectively,³⁰ and it seems therefore quite possible that Γ_γ / Γ for the B¹¹ 8.92-MeV level is considerably closer to unity than 0.84.

The B¹¹ 8.57-MeV Level

The value of R_ω obtained for the $8.57 \rightarrow 0$ transition indicates an $M1, E2$ mixture or an $E1, M2$ mixture. This transition can be pure $E2$ but not pure $M2$, thus the limits on the spin-parity assignment of the 8.57-MeV level from this measurement alone are $J^\pi \leq \frac{5}{2}^+$ or $\frac{7}{2}^-$. If the 8.57-MeV level were $\frac{7}{2}^-$ then the $8.57 \rightarrow 2.14$ transition would be a $M3, E4$ mixture. This is not allowed by the lifetime limit, $\tau < 5 \times 10^{-13}$ sec, which would correspond to a lower limit on the $M3$ strength of about 5000 Weisskopf units. Thus the present results demand $J \leq \frac{5}{2}$.

An $M2$ admixture of the size demanded by the measurement of R_ω if the 8.57-MeV level has even parity seems quite improbable while the $M1, E2$ mixture seems quite reasonable. Thus our results give a strong preference for odd parity and we assign the B¹¹ 8.57-MeV level $J^\pi \leq \frac{5}{2}^-$.

An odd parity assignment to the 8.57-MeV level is in agreement with the Be⁹(He³, p)B¹¹ double-stripping results of Hinds and Middleton²² who reported an intense $L=0$ stripping pattern to the 8.57-MeV level. However, the odd-parity assignment is in disagreement with B¹⁰(d, p)B¹¹ stripping results^{20, 21} which indicate $l_n = 2$ formation of the 8.57-MeV level. This discrepancy and the analogous one for the B¹¹ 8.92-MeV level, already discussed, illustrate the difficulty of making rigorous spin-parity assignments from plane-wave analysis of single and double stripping reactions.

The B¹¹ 7.99- and C¹¹ 7.50-MeV Mirror Levels

The ground-state decays and first-excited state cascades of the B¹¹ 7.99- and C¹¹ 7.50-MeV levels are all

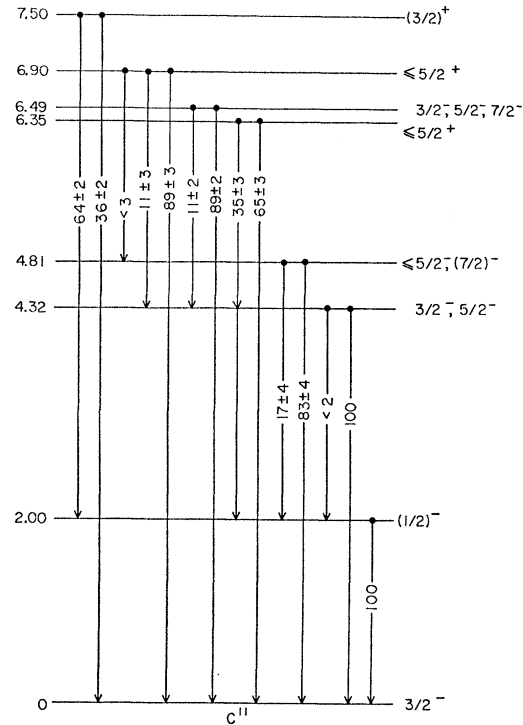


FIG. 10. Level scheme of C¹¹ showing spins, parities and decay modes of those levels studied in the present experiment. The various assignments and branching ratios are obtained as a synthesis of the results of this experiment with those reported from other sources, as explained in the text. Uncertain or less likely assignments are enclosed in parentheses.

predominantly $E1$.³⁴ This fixes the parities of both states as even, confirms the odd-parity assignment of the B¹¹ 2.14-MeV level and fixes the parity of the C¹¹ 2.00-MeV level as odd.

Various investigations^{1, 2} of single and double stripping reactions forming the mirror levels at 7.99 MeV in B¹¹ and 7.50 MeV in C¹¹ have all shown small cross sections and practically isotropic angular distributions. Thus there is no information on the parity of these states from this source.

Both the B¹¹ 7.99 \rightarrow 2.14 and C¹¹ 7.50 \rightarrow 2.00 transitions were observed to have nonzero anisotropies (see Table II) so that both the B¹¹ 7.99- and C¹¹ 7.50-MeV levels have $J > \frac{1}{2}$. Since the B¹¹ 2.14-MeV level has $J^\pi = \frac{1}{2}^-$ and the C¹¹ 2.00-MeV level has $J^\pi = (\frac{1}{2})^-$, the B¹¹ 7.99-MeV level is fixed as $J^\pi = \frac{3}{2}^+$ and the C¹¹ 7.50-MeV level is $J^\pi = (\frac{3}{2})^+$, with $J^\pi = \frac{5}{2}^+$ the only other possibility for this C¹¹ level.

The theoretical ratio of the a_2 coefficients in $W(\theta) = 1 + a_2 p_2(\cos\theta)$ for a $\frac{3}{2} \rightarrow \frac{3}{2}$ transition and a $\frac{3}{2} \rightarrow \frac{1}{2}$ transition is given by³⁵

$$\frac{a_2(\frac{3}{2}, \frac{3}{2})}{a_2(\frac{3}{2}, \frac{1}{2})} = - \left[\frac{0.4 - 1.5492x_1}{0.5 + 1.7321x_2 + 0.5x_2^2} \right] \left[\frac{1 + x_2^2}{1 + x_1^2} \right], \quad (8)$$

³⁴ A preliminary report of the results for the B¹¹ 7.99-MeV level has already been made (see Ref. 5).

³⁵ A. R. Poletti and E. K. Warburton, Phys. Rev. **137**, B595 (1965).

where x_1 and x_2 are the amplitude ratios of $M2$ to $E1$ radiation in the $\frac{3}{2} \rightarrow \frac{3}{2}$ and $\frac{3}{2} \rightarrow \frac{1}{2}$ transitions, respectively. Thus, if both the $\frac{3}{2} \rightarrow \frac{3}{2}$ and $\frac{3}{2} \rightarrow \frac{1}{2}$ transitions are pure $E1$ the expected ratio is -0.8 . From Table II we obtain $-(0.7 \pm 0.4)$ and $-(0.9 \pm 0.8)$ for the ratios $a_2(7.99 \rightarrow 0)/a_2(7.99 \rightarrow 2.14)$ and $a_2(7.50 \rightarrow 0)/a_2(7.50 \rightarrow 2.00)$. Thus the B^{11} 7.99- and C^{11} 7.50-MeV levels both decay by gamma-ray transitions which are consistent with pure $E1$ radiation and the most probable spin assignments to the C^{11} 7.50- and 2.00-MeV levels. Since significant admixtures of $M2$ radiation are not likely the preference for these spin assignments is strengthened.

Morpurgo³⁶ has shown that if charge symmetry is obeyed and Coulomb interactions are neglected then $E1$ transition rates between analog states in mirror nuclei are identically equal. All available evidence indicates that the B^{11} 7.99- and C^{11} 7.50-MeV levels are analog states as are the B^{11} 2.14- and C^{11} 2.00-MeV levels. Thus this prediction applies to the transitions discussed here. This means that the intensity ratios $R(B^{11}) = I(7.99 \rightarrow 2.14)/I(7.99 \rightarrow 0)$ and $R(C^{11}) = I(7.50 \rightarrow 2.00)/I(7.50 \rightarrow 0)$ should be nearly equal since the energy ratios 7.99/5.85 and 7.50/5.50 are practically identical. In actual fact the ratio $R(C^{11})/R(B^{11})$ extracted from Tables III and IV is 1.57 ± 0.18 , rather far from unity. However, we believe a more accurate value for this ratio comes from the magnetic pair spectrometer measurements alone, rather than the averages of all the branching ratios, since in these measurements we obtained $R(B^{11})$ and $R(C^{11})$ simultaneously under the same experimental conditions so that systematic errors cancel to first order in the comparisons of these two ratios. These measurements give $R(C^{11})/R(B^{11}) = 1.34 \pm 0.13$, closer to unity but still significantly different from it.

Morpurgo³⁶ estimated that the effects of Coulomb interactions on $E1$ rates in the region of mass 11 could be, on the average, about 4% for each transition. This estimate is highly model-dependent and only serves to indicate the possibility of large Coulomb corrections. Thus corrections to $R(C^{11})/R(B^{11})$, which involves four transitions, could be large enough to explain the departure of this ratio from unity. Note that the Coulomb corrections to weak transitions can be appreciably larger than this estimate³⁶ and the fact that the cascade transitions to the first excited states compete so well with the ground-state transitions indicates that the latter are most likely weaker than average.

This situation has been discussed previously²² from a different point of view.

The B^{11} 7.30- and C^{11} 6.90-MeV Mirror Levels

The B^{11} 7.30 \rightarrow 0 and C^{11} 6.90 \rightarrow 0 transitions are both predominantly $E1$ so that both these levels have $J^\pi \leq \frac{5}{2}^+$.

The $Be^9(He^3, p)B^{11}$ reaction feeds the B^{11} 7.30-MeV

level weakly³² and gives an angular distribution which cannot easily be interpreted by plane wave stripping theory. The $B^{10}(d, p)B^{11}$ reaction^{20,21} which also feeds the 7.30-MeV level weakly, gives a slight preference for $l_n=2$ and thus even parity for the B^{11} 7.30-MeV level in agreement with present results. The $B^{10}(d, p)B^{11}$ reaction feeds the C^{11} 6.90-MeV level weakly.^{1,2,37} The angular distribution in this reaction has been interpreted³⁷ to indicate $l_p=1$ and thus odd parity for the 6.90-MeV level in disagreement with the present results.

As indicated in Fig. 1 the B^{11} 7.30- and C^{11} 6.90-MeV levels are almost certainly mirror levels. However, if both these levels decay by nearly pure $E1$ transitions as expected, then the branching ratios given for them in Tables III and IV are in very poor agreement. If we carry over the branching ratios for the B^{11} 7.30-MeV level (Table III), suitably adjusted for the energy differences between the mirror transitions, we obtain predictions of $(5 \pm 1)\%$ and $(6 \pm 1)\%$ for the 6.90 \rightarrow 4.32 and 6.90 \rightarrow 4.81 branches, respectively. Here we have taken the two final states in C^{11} to be mirrors of the B^{11} 4.46- and 5.30-MeV levels. These branching ratios are to be compared to²² $(11 \pm 3)\%$ and $< 3\%$, respectively (see Table IV). Since we have checked our results for the decay of the B^{11} 7.30-MeV level by two reactions (Table I), a repetition of the measurement for the C^{11} 6.90-MeV level would appear to be worthwhile.

An assignment of $\frac{1}{2}^+$ to the B^{11} 7.30-MeV level can be shown to be quite improbable from a consideration of the 7.30 \rightarrow 4.46 transition. If this transition were pure $M2$, then the $M2$ transition rate, obtained by combining the lifetime limit $\tau < 5 \times 10^{-13}$ sec with the branching ratio for this transition, would have a lower limit of 5 Weisskopf units. Since such a large $M2$ rate would be quite surprising, the B^{11} 7.30 \rightarrow 4.46 transition is probably not $\frac{1}{2}^+ \rightarrow \frac{5}{2}^-$. This argument is considerably strengthened by the $B^{11}(\gamma, \gamma)B^{11}$ results of Seward³⁸ who observed gamma-ray peaks with energies of 4.4, 5.0, 7.3, and 8.8 MeV in the resonant scattering of gamma rays from B^{11} . The two lower peaks and the upper one are presumably associated with the 4.46-, 5.03-, and 8.92-MeV levels all three of which have mean lifetimes of about 5×10^{-15} sec or shorter.^{1,2} Since the cross section for resonant scattering from the 7.30-MeV level appears to be comparable to that for these three levels it would appear to have a life time considerably shorter than 5×10^{-13} sec, in which case the 7.30 \rightarrow 4.46 transition is certainly not $M2$.

The B^{11} 6.81- and C^{11} 6.35-MeV Mirror Levels

The C^{11} 6.35 \rightarrow 0 transition is predominantly $E1$ so that the C^{11} 6.35-MeV level has $J^\pi \leq \frac{5}{2}^+$. The B^{11} 6.81-MeV level was populated quite weakly in both $B^{10}+d$ and Be^9+He^3 reactions, and its decay modes were not

³⁷ A. N. James, A. T. G. Ferguson, and C. M. P. Johnson, Nucl. Phys. **25**, 282 (1961).

³⁸ E. D. Seward, Phys. Rev. **125**, 335 (1962).

³⁶ G. Morpurgo, Phys. Rev. **114**, 1075 (1959).

studied. However the beta decay from Be¹¹ to both the B¹¹ 7.99- and 6.81-MeV levels is allowed^{4,5} so we can use the $J^\pi = \frac{3}{2}^+$ assignment given to the B¹¹ 7.99-MeV level to fix the Be¹¹ ground state as $J^\pi \leq \frac{5}{2}^+$ and the B¹¹ 6.81-MeV level as $J^\pi \leq \frac{7}{2}^+$. Since both the B¹¹ 6.76-MeV level and the C¹¹ 6.49-MeV level have odd parity (see Fig. 1), the B¹¹ 6.81- and C¹¹ 6.35-MeV levels almost certainly form a mirror pair. The decay modes of these two states are consistent with each other (Figs. 9 and 10).

The angular distribution of the Be⁹(He³,p)B¹¹ reaction to the B¹¹ 6.81-MeV level is reported²² to favor $L=1$ transfer and thus even parity and $J \leq \frac{7}{2}$ for the 6.81-MeV level—the same choice as indicated above. The B¹⁰(d,p)B¹¹ stripping reaction forms the 6.81-MeV level quite weakly and gives no information as to the spin-parity of this level.^{20,21} Likewise the B¹⁰(d,n)C¹¹ reaction^{1,2,37} and the B¹⁰(He³,d)C¹¹ reaction⁸ leading to the C¹¹ 6.35-MeV level have relatively small cross sections and do not give recognizable stripping patterns.

As noted in Fig. 1, the decay modes of the B¹¹ 6.81-MeV level favor $J^\pi = \frac{1}{2}^+$ or $\frac{3}{2}^+$ for this level, primarily because the 6.81 → 2.14 transition would be $M2$ or $E3$ for $J^\pi = \frac{5}{2}^+$ or $\frac{7}{2}^+$. The same argument would apply to the C¹¹ 6.35 → 2.00 transition (if the C¹¹ 2.00-MeV level is $\frac{1}{2}^-$ as is most probable) if it were shown that the (35±3)% branch²² from the C¹¹ 6.35-MeV level were to the 2.00-MeV level and not the C¹¹ 4.32-MeV level.

The B¹¹ 6.76- and C¹¹ 6.49-MeV Mirror Levels

Both the B¹¹ 6.76- and C¹¹ 6.49-MeV levels have been shown to have odd parity and $J \leq \frac{9}{2}$ from the stripping reactions^{1,2,8,20,21,37} B¹⁰(d,p)B¹¹, B¹⁰(d,n)C¹¹, and B¹⁰(He³,d)C¹¹. The double-stripping reaction Be⁹(He³,p)B¹¹ does not appear to have a recognizable stripping pattern.³² Our internal pair correlation measurements indicate practically pure $E2$ for both the B¹¹ 6.76 → 0 and C¹¹ 6.49 → 0 transitions if both initial states have odd parity thus giving $J^\pi \leq \frac{7}{2}^-$. The Li⁷(α,γ)B¹¹ results of Green, Stephens, and Willmott³ fix the spin of the B¹¹ 6.76-MeV level as $J = \frac{7}{2}$. The B¹⁰(p,γ)C¹¹ results of James¹² are consistent with $J^\pi = \frac{7}{2}^-$ for the C¹¹ 6.49-MeV level but do not appear to rule out any other possibility except $J^\pi = \frac{1}{2}^-$.

Thus the various experimental measurements give $J^\pi = \frac{7}{2}^-$ and $J^\pi = \frac{3}{2}^-$, $\frac{5}{2}^-$, or $\frac{7}{2}^-$ for the B¹¹ 6.76- and C¹¹ 6.49-MeV levels, respectively. All evidence is consistent with these two states forming a mirror pair.

The B¹¹ 5.03- and C¹¹ 4.81-MeV Mirror Levels

The internal pair correlation measurements of the B¹¹ 5.03 → 0 and C¹¹ 4.81 → 0 transitions were made with quite poor statistics (Fig. 8). Since both the B¹¹ 5.03- and C¹¹ 4.81-MeV levels are known^{1,2} to have odd parity (Fig. 1), the results serve to limit the spins of both levels by $J^\pi \leq \frac{7}{2}^-$. A more severe restriction is

imposed by the lifetime³³ limit, $\tau < 5 \times 10^{-13}$ sec, which rules out the possibility of an $M3$ transition to the first-excited state in both cases. From this we have $J^\pi \leq \frac{5}{2}^-$ for the B¹¹ 5.03-MeV level and most probably $J^\pi \leq \frac{5}{2}^-$ for the C¹¹ 4.81-MeV level. These results are in agreement with previous work (Fig. 1) which gave $J^\pi = (\frac{1}{2}, \frac{3}{2})^-$ and $J^\pi \leq \frac{9}{2}^-$ for the B¹¹ 5.03- and C¹¹ 4.81-MeV levels, respectively. The branching ratios of this mirror pair are in good accord (Figs. 9 and 10).

The B¹¹ 4.46- and C¹¹ 4.32-MeV Mirror Levels

The ground-state transitions from the odd-parity^{1,2} B¹¹ 4.46- and C¹¹ 4.32-MeV levels are both predominantly $M1$ (Fig. 7) so that both levels have $J^\pi \leq \frac{5}{2}^-$. This is in agreement with the spin-parity assignment of $\frac{5}{2}^-$ given² to the B¹¹ 4.46-MeV level and the range of values ($\frac{3}{2}^- \leq J^\pi \leq \frac{9}{2}^-$) allowed (Fig. 1) for the C¹¹ 4.32-MeV level.

The B¹¹ 2.14- and C¹¹ 2.00-MeV Mirror Levels

As stated previously, the results for the decay of the B¹¹ 7.99- and C¹¹ 7.50-MeV levels confirm the odd parity of the B¹¹ 2.14-MeV level and fix the parity of the C¹¹ 2.00-MeV level as odd also.

B. Comparison with Theory

The Odd-Parity Levels

The odd-parity group of levels arising from the shell-model configuration s^4p^7 (hereafter referred to as p^7) has been investigated theoretically using both the intermediate-coupling model^{7,39} and the unified model.⁴⁰ Both models are able to account fairly well for the first five states of B¹¹ if the B¹¹ 5.03-MeV level has $J^\pi = \frac{3}{2}^-$. The electromagnetic transitions connecting these states have been compared to theory by several authors^{6,7,17} and the nucleon reduced widths of the B¹¹ states for the B¹⁰ ground state have been compared to the intermediate coupling model in some detail²⁰ and found to be in satisfactory agreement. Taken all together, the evidence for the assignment of these five states to the p^7 configuration is quite strong.

An energy gap of about 4 MeV is predicted between the highest of these six states—presumably the B¹¹ 6.76-MeV level—and the next odd-parity level of p^7 which is predicted to have $J^\pi = \frac{5}{2}^-$. Thus, this $\frac{5}{2}^-$ state is predicted to be at an excitation energy of 11 or 12 MeV. Nevertheless, the cross section for the B¹⁰(d,p)B¹¹ (8.92-MeV level) reaction strongly suggests²¹ that the 8.92-MeV level belongs to p^7 , and is the second highest $\frac{5}{2}^-$ level of this configuration. The $M1$ and $E2$ transition strengths connecting the second $\frac{5}{2}^-$ of p^7 to the lower p^7 states have been calculated by Kurath⁷ and compared to the experimental results for the decay modes of the B¹¹ 9.28- and 8.92-MeV levels in an attempt to identify

³⁹ D. Kurath, Phys. Rev. **101**, 216 (1956).

⁴⁰ A. B. Clegg, Nucl. Phys. **38**, 353 (1962).

the $\frac{5}{2}^-$ states in question. At the time this comparison was made the spins of the B^{11} 4.46- and 6.76-MeV levels were not known so that it is now worthwhile to reconsider this comparison. Also, the 9.28-MeV level is now known to have even parity (Fig. 1) so that the B^{11} 8.57- and 8.92-MeV levels are the only two candidates for the second $\frac{5}{2}^-$ level below an excitation energy of 9.3 MeV.

The second $\frac{5}{2}^-$ level of p^7 is predicted to have a negligible branch ($<0.5\%$) to the $\frac{1}{2}^-$ level at 2.14 MeV. This is in strong disagreement with the decay of the B^{11} 8.57-MeV level, but consistent with the decay of the 8.92-MeV level (Fig. 9). Likewise the reduced width of the 8.57-MeV level for the B^{10} ground state is quite small^{20,21} in poor agreement with that expected for the second $\frac{5}{2}^-$ level while the reduced width of the 8.92-MeV level is in good agreement for a/K near 6.²¹ Thus, we conclude that the 8.57-MeV level is quite probably not this $\frac{5}{2}^-$ state and we consider the decay of the 8.92-MeV level in more detail.

Using the results given by Kurath,⁷ we find that the decay modes of the 8.92-MeV level (Fig. 9) are in fair agreement with that predicted for the second $\frac{5}{2}^-$ state if $a/K > 5$, and in excellent agreement in the jj limit for which the only non-negligible branches are predicted to be to the ground state (96%) and 4.46-MeV level (4%). The next best agreement comes at $a/K = 5.8$, where branches of 1% and 2% are predicted to the 6.76- and 4.46-MeV levels with the remaining 97% going to the ground state. Here we identify the ground state, 4.46-MeV level, and 6.76-MeV level, as the lowest $\frac{3}{2}$, $\frac{5}{2}$, and $\frac{7}{2}$ states of p^7 . Note that there is some disagreement as to the branching ratio of the $8.92 \rightarrow 6.76$ transition (Table III); the results of Green, Stephens, and Willmott,³ for instance, give perfect agreement between the decay modes of the 8.92-MeV level and the predictions for the second $\frac{5}{2}^-$ level near $a/K = 5.8$.

The total radiative width Γ_γ of the second $\frac{5}{2}^-$ state is predicted to vary between 0.44 eV ($a/K = 0$) and 4.9 eV ($a/K = 7.5$) with a value of 3.8 eV at $a/K = 6$. This prediction is consistent with our limit $\Gamma_\gamma \geq 0.15$ eV. We conclude that all the available evidence is consistent with an identification of the B^{11} 8.92-MeV level with the second $\frac{5}{2}^-$ level of p^7 if we are allowed freedom in our choice of the spin-orbit strength a/K .

The B^{11} 8.57-MeV level, which has $J = \frac{1}{2}, \frac{3}{2},$ or $\frac{5}{2}$ and almost certainly odd parity, is the only remaining B^{11} level below 9.3-MeV excitation which can be assigned to an odd-parity configuration. The distinguishing characteristics of this state are a very small reduced width for the B^{10} ground state,^{20,21} a relatively large two-nucleon parentage coefficient for the Be^9 ground state,³² a large $E2$ component in the $8.57 \rightarrow 0$ gamma-ray transition (Fig. 8), a large gamma-ray branch to the B^{11} 2.14-MeV level, and small branches to both the 4.46- and 5.03-MeV levels.

It seems probable that the 8.57-MeV level belongs

predominantly to one of three configurations. These are (1) p^7 , (2) $p^6 f_{7/2}$, i.e., to the configuration formed by weak coupling a $f_{7/2}$ nucleon to the B^{10} ground state, (3) $p^5(2s, 1d)^2$, i.e., to the configuration formed by coupling two nucleons in the nearly degenerate $2s_{1/2}, 1d_{5/2}$ orbits to the Be^9 ground state. In the absence of detailed theoretical calculations the definite assignment to the B^{11} 8.57-MeV level to one of these three configurations is not possible, and would be difficult in any case without more experimental information such as a definite spin determination of this level.

The Even-Parity Levels

There are five known even-parity levels in B^{11} below an excitation energy of 9.3 MeV. The highest two of these at 9.19 and 9.28 MeV have been explained quite convincingly²⁰ as arising from the weak coupling of a $2s_{1/2}$ nucleon to the B^{10} ground state. The remaining three levels at 6.81, 7.30, and 7.99 MeV all have startlingly small reduced widths for the B^{10} ground state.^{20,21} Only for the 7.30-MeV level is there a suggestion of a stripping pattern in the $B^{10}(d, p)B^{11}$ reaction²¹ and the $l_n = 2$ reduced width which is extracted is only about $\frac{1}{10}$ of the single-particle value.²¹ Thus if these three states arise from p^6s or p^6d none of them appear to have the B^{10} ground state as its major parent. It would seem then that these three states are formed predominantly by coupling of a $2s_{1/2}$ or $1d_{5/2}$ nucleon to a p^6 core which does not resemble the B^{10} ground state or arise from configurations other than p^6s and p^6d . The only such configuration which seems likely is $p^4(2s, 1d)^3$, i.e., the configuration formed by raising three nucleons from the p shell into the $2s$ and $1d$ shells. The lowest state of this configuration is predicted⁴¹ to be predominantly $(2s_{1/2})^3$ coupled to a $0^+, p^4$ core, with a predicted excitation energy for this $\frac{1}{2}^+$ state in B^{11} of 10.6 MeV. This $\frac{1}{2}^+$ state would have a negligibly small two-nucleon parentage coefficient for the Be^9 ground state. The B^{11} 6.81-MeV level is the only even-parity state of B^{11} below an excitation energy of 9.3 MeV for which $J^\pi = \frac{1}{2}^+$ is likely (see Fig. 9). The predicted energy of the $\frac{1}{2}^+, p^4(2s, 1d)^3$ state could conceivably be in error by $10.6 - 6.8 = 3.8$ MeV; but the $L = 1$ double stripping pattern observed³² in the $Be^9(He, p)B^{11}$ reaction leading to the B^{11} 6.81-MeV level would seem to demand a significant contribution from some other configuration with a nonzero two-nucleon parentage coefficient for the Be^9 ground state.

In the region of mass 11 the $2s_{1/2}$ shell appears at a lower energy than the $1d_{5/2}$ shell (see, e.g., Be^9 and C^{13}) so that p^6s appears more probably the origin of these three states than p^6d . In the weak coupling scheme we can have a $\frac{1}{2}^+, \frac{3}{2}^+$ pair of states formed by coupling $2s_{1/2}$ to the 1^+ first-excited state of B^{10} at 0.72 MeV. These two states could correspond to the B^{11} 6.81-MeV

⁴¹ W. W. True and E. K. Warburton, Nucl. Phys. 22, 426 (1961).

level and one or another of the 7.30- and 7.99-MeV levels. If so the third state (either the 7.99- or 7.30-MeV level) would have, in this scheme, a higher B¹⁰ state for a core.

The B¹¹ 7.30-MeV level is distinguished from the 6.81- and 7.99-MeV levels by virtue of the observed beta decay from Be¹¹ to the latter two states but not to it.^{4,5} The Be¹¹ ground state is expected, but not proven, to have $J = \frac{1}{2}$.⁴² Thus, an obvious explanation for this difference is that the B¹¹ 7.30-MeV level has $J^\pi = \frac{5}{2}^+$. If this is so and if this state arises predominantly from p^6s it would necessarily have a $(J^\pi, T) = (2^+, 1)$ or $(3^+, 0)$ p^6 core. An intriguing possibility is that the B¹¹ 6.81-MeV level arises mainly from a $2s_{1/2}$ nucleon coupled to a $(J^\pi, T) = (0^+, 1)$ p^6 core and the 7.30- and 7.99-MeV levels are the $\frac{5}{2}^+$ and $\frac{3}{2}^+$ states arising from a $2s_{1/2}$ nucleon coupled to a $(J^\pi, T) = (2^+, 1)$ p^6 core. If this picture were even approximately true it would imply some mechanism for lowering those p^6s states with a $T = 1$ p^6 core relative to those with a $T = 0$ p^6 core. Such a situation may exist in N¹⁵ where the lowest $\frac{1}{2}^+$ state is calculated to have a predominantly $(J^\pi, T) = (0^+, 1)$ p^{10} core rather than a $(J^\pi, T) = (1^+, 0)$ p^{10} core⁴³; whereas, the lowest $(J^\pi, T) = (0^+, 1)$ state in N¹⁴ is 2.31 MeV above the $(J^\pi, T) = (1^+, 0)$ ground state.² There can be two states in B¹¹ arising from coupling a $2s_{1/2}$ nucleon to a $(J^\pi, T) = (0^+, 1)$ p^6 core. One of these is the $(J^\pi, T) = (\frac{1}{2}^+, \frac{1}{2})$ state already tentatively identified as the B¹¹ 6.81-MeV level and the other has $(J^\pi, T) = (\frac{1}{2}^+, \frac{3}{2})$. The latter state is presumably the analog of the Be¹¹ ground state and its excitation energy can be estimated from the measured⁴⁴ energy difference between B¹¹ and Be¹¹, 11.510 ± 0.015 MeV, by applying a correction for the Coulomb energy difference between analog states in nuclei (Z, A) and $(Z-1, A)$. We use the semiempirical procedure of Woods and Wilkinson⁴⁵ to estimate this correction and find 12.62 MeV for the estimated excitation energy of the lowest $T = \frac{3}{2}$ level in B¹¹. A state has been observed⁴⁶ at 12.565 ± 0.012 MeV

in B¹¹ and assigned as most probably the lowest $T = \frac{3}{2}$ level in B¹¹. Thus, if the 12.57- and 6.81-MeV levels are the $T = \frac{3}{2}$ and $\frac{1}{2}$ states in question the separation between them is about 5.8 MeV. This separation seems reasonable when compared to that of other p^6s states which differ only by their isotopic spin. For instance the separation between the lowest $T = \frac{3}{2}$ state in N¹⁵ and the $(J^\pi, T) = (\frac{1}{2}^+, \frac{1}{2})$ 5.30-MeV level of N¹⁵ discussed previously is about $11.6 - 5.3 = 6.3$ MeV.²

In order to check further this possible identification of the B¹¹ 6.81-MeV level, we have calculated the ft value for the beta decay from a $T = \frac{3}{2}$, $J^\pi = \frac{1}{2}^+$ Be¹¹ state to a B¹¹ $T = \frac{1}{2}$, $J^\pi = \frac{1}{2}^+$ state for the simple model of a $2s_{1/2}$ nucleon coupled to a $(J^\pi, T) = (0^+, 1)$ p^6 core. The result is $\log ft = 3.4$. The experimental $\log ft$ value^{4,5} for the beta decay of Be¹¹ to the B¹¹ 6.81-MeV level is 5.93; thus this model gives a poor description of the B¹¹ 6.81-MeV level and/or the Be¹¹ ground state.⁴⁷ We conclude that if the B¹¹ 6.81-MeV level has $J^\pi = \frac{1}{2}^+$ then it is almost certainly not a nearly pure $\frac{1}{2}^+$, $p^4(2s, 1d)^3$ state or the $\frac{1}{2}^+$ state formed by a $2s_{1/2}$ nucleon coupled to a 0^+ , p^6 core. It could conceivably be described as a $2s_{1/2}$ nucleon coupled to a 1^+ , p^6 core or it could have significant admixtures of two or even all of these three configurations.

It would appear that considerably more experimental work is needed before the origin of the B¹¹ 6.81-, 7.30-, and 7.99-MeV levels is understood. Of first importance is a determination of the spins of the lower two levels. Valuable information could also be gained from a study of the Be¹⁰(d, n)B¹¹ or Be¹⁰(He³, d)B¹¹ reactions.

VI. ACKNOWLEDGMENTS

We wish to thank E. Windschauer for calculating the theoretical curves of $R_\omega(l)$ as functions of internal-pair transition energies. The efforts of I. Cole and J. Milazzo in adapting the various data handling procedures for computer operation are acknowledged.

⁴⁷ It is interesting to note that the same calculation can be applied to the beta decay of C¹⁵ assuming that the C¹⁵ ground state and N¹⁵ 5.30-MeV level have a common $p^{10}(J^\pi, T) = (0^+, 1)$ core. The experimental $\log ft$ value for C¹⁵ β^- N¹⁵ (5.30-MeV level) is 4.07 ± 0.03 [D. E. Alburger, A. Gallmann, and D. H. Wilkinson, Phys. Rev. **116**, 939 (1959)] which is intermediate between $\log ft = 3.4$ and the full intermediate coupling result, $\log ft = 4.8$, obtained by Halbert and French (Ref. 43).

⁴² I. Talmi and I. Unna, Phys. Rev. Letters **4**, 469 (1960).

⁴³ E. C. Halbert and J. B. French, Phys. Rev. **105**, 1563 (1957).

⁴⁴ D. J. Pullen, A. E. Litherland, S. Hinds, and R. Middleton, Nucl. Phys. **36**, 1 (1962).

⁴⁵ J. B. Woods and D. H. Wilkinson, Nucl. Phys. **61**, 661 (1965).

⁴⁶ D. E. Grace, J. H. McNally, and W. Whaling, Bull. Am. Phys. Soc. **8**, 486 (1963).